

American University in Cairo

AUC Knowledge Fountain

Theses and Dissertations

6-1-2016

Development and characterization of environmentally friendly high performance polymeric nanocomposite blends of Cellulose Acetate, Poly(Lactic acid) and Polyurethane

Sara Moustafa

Follow this and additional works at: <https://fount.aucegypt.edu/etds>

Recommended Citation

APA Citation

Moustafa, S. (2016). *Development and characterization of environmentally friendly high performance polymeric nanocomposite blends of Cellulose Acetate, Poly(Lactic acid) and Polyurethane* [Master's thesis, the American University in Cairo]. AUC Knowledge Fountain.

<https://fount.aucegypt.edu/etds/271>

MLA Citation

Moustafa, Sara. *Development and characterization of environmentally friendly high performance polymeric nanocomposite blends of Cellulose Acetate, Poly(Lactic acid) and Polyurethane*. 2016. American University in Cairo, Master's thesis. *AUC Knowledge Fountain*.

<https://fount.aucegypt.edu/etds/271>

This Thesis is brought to you for free and open access by AUC Knowledge Fountain. It has been accepted for inclusion in Theses and Dissertations by an authorized administrator of AUC Knowledge Fountain. For more information, please contact mark.muehlhaeusler@aucegypt.edu.

AMERICAN UNIVERSITY IN CAIRO
SCHOOL OF SCIENCE AND ENGINEERING

Development and Characterization of Environmentally
Friendly High Performance Polymeric Nanocomposite
Blends of Cellulose Acetate, Poly(Lactic acid) and
Polyurethane

A Thesis Submitted to
Masters of Science in Nanotechnology Program
In partial fulfillment of the requirements for
The degree of Master of Science

By:

Sara Ayman Moustafa

Under the supervision of: Prof.
Tarek Madkour (Advisor)

Department of Chemistry, The American University in Cairo

Acknowledgement:

First and foremost, I would like to express my sincere appreciation to my supervisor, Professor Dr. Tarek Madakour. For all his patience, guidance and putting up with me for long times. Without him believing in me and his never ending support I wouldn't have make it this far. His scientific and moral support for me and my colleagues is an example of a true mentor.

Special thanks to Dr. Adham Ramadan as The Dean of Graduate studies for his unlimited support and encouragement; and for being a great professor as I was honored to attend two of his classes which had a deep impact on me and my scientific work.

My ultimate appreciation for the whole Chemistry department; Mr. Mahmoud abdel Moez, Mr. Emad Raafat and Mr. Ahmed Omia for their dedication and sincere prompt help to me and my colleagues. Eng. Ahmed el Ghazaly in the STRC center for his continuous help and support.

I would like to express my great gratitude for my dear friend Worood El Mehelmy, for her great, unbelievable support and efforts. I wouldn't have come to the end of this journey without her push and sincere encouragement, I am lucky to have her as friend. My lab colleagues, who have helped me throughout the whole process. Ahmed Hamdy, Samar Fadl, Ghada Taher, Salma Fouad. Thank you all, I will always be grateful.

I would like to specially thank my parents and my sisters, for believing in me and having my back all these years. For their unconditional love and support through all the hard times I have been through. For always encouraging me and believing that I can always do better. My dear husband who have put up with me through all these years, without his continuous support and encouragement I wouldn't have made it. My dear son Hassan, I wish all the best and I hope you'd be proud of me one day.

Finally, I would like to thank the American University in Cairo for giving me such a unique opportunity to study a new, promising field.

Abstract:

The discovery of biopolymers, several years ago have received great interest as biodegradable-biocompatible material for several applications. Cellulose acetate, poly (lactic acid) and polyurethane, are widely employed biopolymers owing to their interesting characteristics. However, CA and PLA exhibit poor mechanical properties. Nanoreinforcement is incorporated into CA/PLA and CA/PU matrices in order to overcome their brittle nature and to improve their properties.

This research focused studying the effect of blending PLA and PU with CA at different ratios to form new CA/PLA and CA/PU blend using solvent casting method. The second aspect of this study is studying the incorporation of nanoreinforcement material, functionalized graphene nanoplatelets, at different ratios to form new CA/PLA/0.5wt%GNPS-COOH and CA/PU/0.5wt%GNPS-COOH nanocomposites using solvent casting method. All prepared samples were investigated through stress-strain measurements, FT-IR, DSC, TGA, SEM and dry thermal degradation. GNPS-COOH nanocomposites exhibited the best mechanical behavior for all samples. TGA analysis revealed a slight improvement in the thermal stability. DSC analysis showed no effect on thermal stability. SEM showed uniform distribution of the nanofiller in the matrices. The biodegradation of the nanocomposites when placed in an oven at 100°C investigated and it was observed that complete degradation occur at day 14.

Contents

	Page
Acknowledgement	i
Abstract	ii
List of Tables	vi
List of Figures	vii
List of Abbreviations	x
1. Introduction	1
1.1. Biopolymers.....	1
1.1.1. Poly(lactic acid)	1
1.1.2. Polyurethane	2
1.1.3. Cellulose acetate	3
1.2. Reinforcement Materials.....	4
1.2.1. Graphene Nanoplatelets.....	5
2. Motivation	6
2. Literature Review	7
2.1. Nanocomposites	7
2.1.1. Poly(lactic acid)-based- nanocomposites.....	7
2.1.2. Polyurethane-based-nanocomposites.....	8
2.1.3. Cellulose acetate-based-nanocomposites.....	9
2.1.4. Natural polymers/ Carbon-based Nanocomposites	10
2.1.4.1. Polypropylene/ Graphene Nanocomposites	10
2.1.4.2. Polyurethane/Graphene Nanocomposites	10
2.1.4.3. PolyLactic Acid/ Graphene Nanocomposites	11
2.1.4.4. Cellulose acetate/Graphene Nanocomposites	12
3. Experimental	13
3.1. Materials	13
3.2. Methods	13
3.2.1. Preparation of Pure Polymers	13
3.2.2. Preparation of CA/PLA or CA/PU Composites	14
3.2.3. Preparation of GnPs-COOH-Based Nanocomposites	14
3.2.4. Preparation of CA/ PLA or CA/PU /GnPs-COOH Nanocomposites.....	15
3.3. Characterization Techniques.....	15
3.3.1. Fourier Transform Infra-Red Spectroscopy (FTIR)	15
3.3.2. Scanning Electron Microscopy (SEM)	16

3.3.3. Thermogravimetric Analysis (TGA)	17
3.3.4. Differential Scanning Calorimetry (DSC)	18
3.3.5. Stress-Strain Measurements	19
3.3.6. Dry Thermal Degradation Test	20
4. Results and Discussions	21
4.1 Investigation of the molecular interaction of the Prepared Nanocomposites	21
4.1.1 Fourier Transform Infrared Analysis	21
4.2. Investigation of the Nanofiller Dispersion throughout the polymeric matrices of the Prepared Nanocomposites	27
4.2.1. Scanning Electron Microscopy Analysis	27
4.3. Investigation of the Thermal Properties of the Prepared Nanocomposites	29
4.3.1. Thermogravimetric Analysis	29
4.3.2 Differential Scanning Calorimetry analysis	34
4.4. Investigation of the Mechanical Properties of the Prepared Nanocomposites	38
4.4.1. Stress/ Strain Measurements	38
4.4.1.1. Neat CA, PLA and PU	38
4.4.1.2. PLA/CA Composites	40
4.4.1.3. PU/CA Composites	42
4.4.1.4. PLA/CA/GnPs-COOH Nanocomposites	44
4.4.1.5. PU/CA/GnPs-COOH	46
4.4.2. Dry Thermal degradation test	48
4.4.2.1. Stress/Strain Measurements	49
4.4.2.2. CA, PLA and PU	51
4.4.2.3. PLA/CA composites	52
4.4.2.4. PU/CA composites	52
4.4.2.5. CA, PLA and PU with GnPs-COOH nanocomposites	53
4.4.2.6. PLA/CA/GnPs--COOH	56
4.4.2.7. PU/CA/GnPs-COOH	57
5. Conclusion and Future Work	58
References	64

List of Figures

Figure No.	Title	Page
1.1	Chemical Structure of Poly (lactic acid)	2
1.2	Chemical Structure of Polyurethane.	3
1.3	Chemical Structure of Cellulose Acetate	4
2.1	Scanning Elctron Microscopy	16
2.2	Thermogravimetric analysis instrument	18
2.3	Differential Scanning Calorimetry instrument	17
4.1	FT-IR spectra of neat CA in comparison with the CA/GnPs-COOH Nanocomposite	22
4.2	FT-IR spectra of neat PLA in comparison with PLA/GnPs-COOH Nanocomposite	23
4.3	FT-IR spectra of neat PU in comparison with the PU/GnPs-COOH Nanocomposite	24
4.4	FT-IR spectra of 60% PLA/CA in comparison with PLA/CA/GnPs-COOH Nanocomposite	25
4.5	FT-IR spectra of 80%PLA/CA in comparison with PLA/CA/GnPs-COOH Nanocomposite	25
4.6	FT-IR spectra of 60%PU/CA in comparison with PU/CA/GnPs-COOH Nanocomposite	26
4.7	FT-IR spectra of 80%PU/CA in comparison with PU/CA/GnPs-COOH Nanocomposite	27
4.8	SEM micrographs of CA/GnPs-COOH, PLA/GnPs-COOH, PU/GnPs-COOH, PLA/CA/GnPs-COOH and PU/CA/GnPs-COOH	28
4.9	TGA thermograms of neat CA in comparison to CA/GnPs-COOH	29
4.10	TGA thermograms of neat PLA in comparison to PLA/GnPs-COOH	30
4.11	TGA thermograms of neat PU in comparison to PU/GnPs-COOH	30
4.12	TGA thermograms of PLA/CA/GnPs-COOH nanocomposite in comparison with PLA/GnPs-COOH and CA/GnPs-COOH	31
4.13	TGA thermogram of PU/CA/GnPs-COOH	33

Figure No.	Title	Page
4.14	DSC thermogram for CA/GnPs-COOH	35
4.15	DSC thermogram for PLA/GnPs-COOH	36
4.16	DSC thermogram for PU/GnPs-COOH	36
4.17	DSC thermogram for PLA/CA/GnPs-COOH	36
4.18	DSC thermogram for PU/CA/GnPs-COOH	37
4.19	Stress-strain isotherm of neat CA	38
4.20	Stress-strain isotherm of neat PLA	39
4.21	Stress-strain isotherm of neat PU.	40
4.22	Stress-Strain isotherm of PLA/CA composites at different ratios	41
4.23	Stress-Strain isotherm of PU/CA composite at different ratios	43
4.24	Stress-strain isotherms of PLA/CA/GnPs-COOH nanocomposites	45
4.25	Stress-Strain isotherm of PU/CA/GnPs-COOH nanocomposites	47
4.26	Stress-strain isotherm of dry thermal degradation test for neat CA	49
4.27	Stress-strain isotherm of dry thermal degradation test for neat PLA	50
4.28	Stress-strain isotherm of dry thermal degradation test for neat PU	51
4.29	Stress-strain isotherm of dry thermal degradation test for blend of 60%PLA	52
4.30	Stress strain curves of dry thermal degradation for blends of 60%PU	53
4.31	Stress-strain isotherm of dry thermal degradation test for CA/GnPs-COOH	54
4.32	Stress-strain isotherm of dry thermal degradation test for PLA/GnPs-COOH	55
4.33	Stress-strain isotherm of dry thermal degradation test for PU/GnPs-COOH	56
4.34	Stress-strain isotherm of dry thermal degradation test for 60%PLA/GnPs-COOH	56
4.35	Stress-strain isotherm of dry thermal degradation test for 60%PU/ GnPs-COOH	57

List of Tables

Table No.	Title	Page
4.1	neat CA,PLA and PU in comparison to CA, PLA and PU nanocomposites	31
4.2	Characteristic temperatures at different ratios of PLA/CA/GnPs-COOH	32
4.3	Characteristic temperatures at different ratios of PU/CA/GnPs-COOH	34
4.4	Ultimate mechanical properties for neat CA and PLA/CA composite at different ratios	42
4.5	Ultimate mechanical properties for PU/CA composites	43
4.6	Ultimate mechanical properties for CA/PLA/GnPs-COOH composites and CA/PLA blends at different ratios	46
4.7	Ultimate mechanical properties for PU/CA/GnPs-COOH nanocomposites.	48

List of Abbreviations

BP	: Biopolymers
CA	: Cellulose acetate
CNC	: Cellulose nanocrystals
CNT	: Carbon nanotubes
CNTCOOH	: carboxylic group-functionalized carbon nanotubes
DCM	: Dichloromethane
DSC	: Differential Scanning Calorimetry
EPO	: Epoxidized Palm Oil
FT-IR	: Fourier Transform Infra-Red Spectroscopy
GNP	: Graphene Nanoplatelets
GnPs-COOH	: Carboxylic group-Functionalized Graphene Nanoplatelets
GO	: Graphene Oxide
MWCNT	: Multi-Wall Carbon Nanotubes
NG	: Natural Graphite
PBS	: Poly butylene succinate
PDLA	: Poly (D-Lactic Acid)
PEO	: Polyethylene oxide
PLA	: Poly (Lactic Acid)
PLLA	: Poly (L-lactic acid)
PNC	: Polymer Nanocomposites
PP	: Polypropylene
PU	: Polyurethane
rGO	: Reduced Graphene Oxide
SEM	: Scanning electron microscopy
SWCNTs	: Single-Wall Carbon Nanotubes
TGA	: Thermogravimetric Analysis

Chapter One:

Introduction

1. Introduction:

1.1. Biopolymers:

Biopolymers discovered several years ago have received great interests as biodegradable, biocompatible material for several applications; especially in the biomedical and food industry. (1,2) Biopolymers can be either produced from renewable sources or extracted from natural ones as well as crude oil. (3) They are categorized according to their production techniques into four classes. (4) Firstly, natural biopolymers are those extracted from natural raw materials such as starch as well as cellulose. Secondly, synthetic biopolymers are those synthesized by chemical processes from bio-derived monomers such as poly (lactic acid). Thirdly, those are produced either from genetically modified bacteria or any other microorganism such as bacterial cellulose, pullan, xanthan, and polyhydrobutyrate. Fourthly, polymers that are produced from crude oils such as polyvinyl alcohol, aromatic polyesters and aliphatic polyesters. (3,4)

Recently, industrial attention has been paid to aliphatic polyesters with reactive groups such as poly (lactic acid) (PLA) as they are biodegradable and biocompatible polymers (5). PLA was widely investigated in several applications such as hernias, tissue engineering, artificial ligaments and surgical implant engineering. It is used in the production process of nanoparticles used in drug delivery as well. Although, they are easily affected and hydrolyzed by moisture, their hydrolyzed products are harmless and nontoxic; this makes them more attractive biocompatible materials. (3,4,5)

1.1.1. Poly(Lactic acid): (PLA)

PLA shown in *Figure 1.1* is biodegradable linear aliphatic thermoplastic polyester produced from renewable resources. (6) PLA is synthesized by ring-opening polymerization of lactide. (7) Lactic acid monomers used in the polymerization process are obtained from fermentation of sugar feed stocks. PLA is thermally unstable; it rapidly loses its weight as a result of thermal treatment that is done at processing temperature. (8) The melting temperature of PLA is about 173-178° while glass transition temperature is 50-60°C Thermal degradation occurs mainly by random main chain scissions. Its low glass transition temperature limits its use in thermally processed packaging.(9)

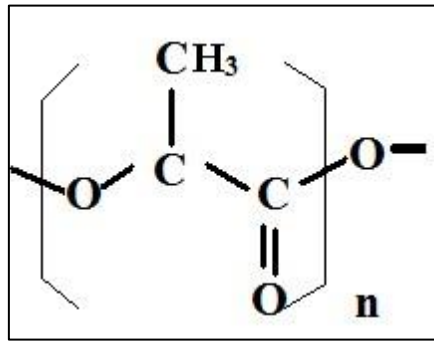


Figure 1.1 Chemical Structure of Poly (lactic acid).

It takes a long period of time for PLA to be degraded in soil as PLA-degraders microorganisms are not widely found in the soil, which further makes the PLA less prone to microbial attack compared to other polymers. (10) PLA production emits less CO₂; which is considered the major greenhouse gas contributes in changing the global climate, compared to other polymers. (11) However, it suffers from major drawbacks which are low deformation break and significant high prices. Lots of trials were carried out to improve the properties of PLA in order to compete with other polymers with lower cost and more flexible properties. (12) Those trials were either done by blending the PLA with other biocompatible polymers or by modifying it with plasticizers to adjust its crystallinity or by the addition of nanofillers. (13) The use of nanofillers is of great interest since the addition of minute amounts of nanofillers (wt. %), can drastically improve its properties while maintain the key PLA properties intact. (14) However, interfacial interaction and good dispersion with the polymer matrix is greatly important as for those improvements to be of significance. (15,16,17)

1.1.2. Polyurethane: (PU)

Polyurethane (PU) is considered a unique polymeric material. As it possess a wide range of chemical and physical properties. (18) It consists of three constituents. diisocyanate, chain extender and polyol as shown in **Figure 1.2**. Those three constituents react to form a segmented polymer that consists of hard and soft segments. (19) The soft segment is derived from the polyols such as polyether and polyester polyols however; the hard ones are formed from the diisocyanate and the chain extender. (20) The dominant segments' nature plays a crucial role in the biodegradation of polyurethane. Therefore, choosing the appropriate segment can tailor the degradation.

Polyether based polyurethane are usually resistant to biodegradation. (21) While polyester based polyurethane is more likely to be readily biodegraded. The nature of the chain extender and its influence were studied and it was found that, introducing a chain extender with hydrolysable ester linkage will allow the hard segment part of the polyurethane to be degradable. (22-24)

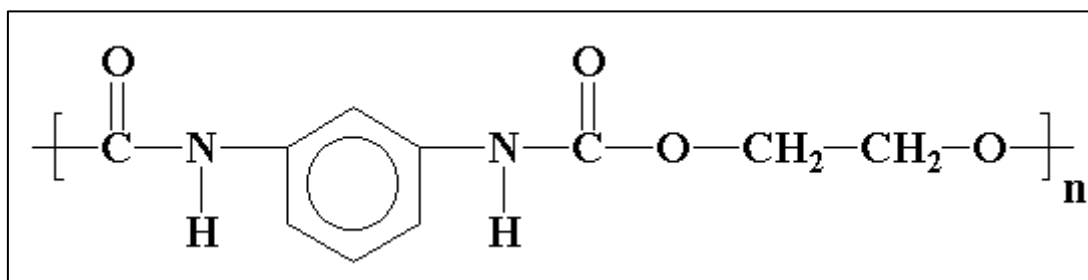


Figure 1.2 Chemical Structure of Polyurethane.

1.1.3. Cellulose Acetate: (CA)

Cellulose is the fundamental component of fiber wall. It shares almost 40-50% of the dry mass of the woods. (25) It consists of linked sugar molecules of long chain which gives the wood its prominent strength. It is considered the basic building block for many industries such as textiles and for fiber based papers. Cellulose acetate (CA) is the ester form of cellulose as shown in *Figure 1.3*. It is a thermoplastic, amorphous polymer. CA is odorless, tasteless and non-toxic available either as white powder or flakes. It is produced from the cellulose found in the wood pulp through direct acetylation. However, this method has a major drawback; the uneven reactivity of the cellulose. (26)

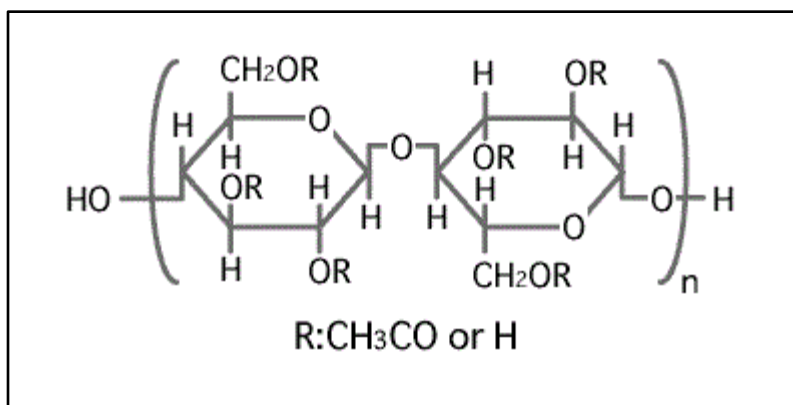


Figure 1.3 Chemical Structure of Cellulose Acetate.

CA has a high glass transition temperature which limits its thermal processing. However, this problem can be overcome through its blending with other flexible

polymers- It is a hydrophilic polymer, therefore it possess an excellent absorptive properties as well as liquid transportation. CA can be used in many applications; a component in adhesives, frame material for eyeglasses and as a film base in photography. It is highly known in the paper production, through the use of cellulose acetate nanofibers produced by electrospinning. (27)

It has been reported that CA properties can be improved due to being reinforced by other materials such as graphene. The incorporation of graphene with a function group -COOH, has shown an improvement in the brittleness of the hybrid fibers as well as increasing the young's modulus 3.7 times higher than pure CA nanofibers. When graphene flakes were added to CA matrix it showed an improvement in tensile strength of nanocomposite by about 31.8% compared to unmodified films. (26,27)

1.2. Reinforcement Materials:

Carbon as a remarkable element is widely known for its extraordinary ability of combining itself with other chemical elements in various ways. (28) The carbon atoms are arranged in a hexagonal lattice in each layer, with the distance between planes is found to be 0.335 nm and separation of 0.142 nm. Graphene has been tested to be the strongest material on Earth as well as carbon nanotubes (CNT). (29) Graphite is said to be one of the allotropes of carbon that possesses a planar, layered structure. (30) Nanocomposite is a multi- component material in which one of the phases is dispersed in second one. Ceramic fillers are typically used to increase the stiffness and reduce cost. However, using these rigid particles has not shown the optimum results desired. (31) On the other hand, the outstanding properties of graphene, carbon nanoplatelets and carbon nanotubes can be exploited by incorporation of such nanofillers into the matrices to form nanocomposites. There are several methods used for manufacturing nanocomposites but the real struggle is to disperse the nanofiller as it is a crucial factor for tuning their properties. (32,33,34)

1.2.1. Graphene Nanoplatelets: (GnPs)

Carbon-based materials such as graphene, carbon nanotubes and nanofibers have drawn worldwide attention lately due to their outstanding mechanical, electrical and thermal properties. (35) However, they have shown major drawbacks in their production; high fabrication cost and low production rate. On the other hand, graphene nanoplatelets possess all of the previous advantages in addition to their low fabrication

cost using top down approach. (36) It consists of few layers of graphene and it can be produced either by microwave radiation technique followed by pulverization using sonication or ball milling or by thermal expansion of acid intercalated natural graphite. Graphene is considered the elementary structure of graphite. It is composed of sp^2 carbon atoms that are arranged in a flat honey comb structure. (37) The theoretical elastic modulus of a single graphene sheet is about 1 TPa while the young modulus is about 1060 MPa. Its electrical conductivity is 50×10^6 s/cm, to negate the Van der Waals force of attraction between the nanoplatelets is a major factor to achieve better dispersion, which will happen by selecting a suitable medium. It possesses an extremely high surface area as well as its high mechanical strengths. (38) Graphene is a hydrophobic in nature, and its stable dispersion in water can only be obtained with the use of proper surfactant. However, graphene oxide is hydrophilic in nature as it contains polar groups in its structure. However, their presence reduce the thermal stability of the nanomaterial, they promote its interaction with various polymeric matrices. These polar groups provide sites for covalent bonding of graphene with polymers such as PU. The hydroxyl functions of graphene will react with the isocyanate termini of PU to form PU/graphene chemical hybrids. (39) Moreover, Graphene can be used as a functional reinforcement for polymers to be used in aircraft, automotive, packaging and many more. Adding a functional group such as hydroxyl, carboxyl, and epoxy on the basal plane of graphene will help in enhancing the interaction with the polymer matrix. (40) This better interaction between the polymer and the nanofiller will lead to exfoliation of the nanofiller with in the matrix which will surely improve the thermal, electrical, electronic and mechanical properties of the polymer. (41)

The dispersion of GnP as nanofiller inside polymeric matrices was studied intensively during past years. A high degree of platelet agglomeration will take place inside the GnP/polymer composited when the attractive forces dominate. (42) It is essential to have a homogenous dispersion and strong interfacial interaction between the polymer matrices and the graphene basal plane to achieve the targeted nanocomposite properties.(43,44)

2. Motivation:

Biopolymers may provide an excellent alternative to petroleum-based polymers but their poor mechanical, thermal and barrier performance may form an obstacle to their full utilization. (45) This work focuses on the development of new biodegradable polymer nanocomposites with enhanced thermal and mechanical properties. Using biodegradable polymeric blends of Poly (Lactic acid) and polyester-based polyurethane with cellulose acetate for the development of these novel nanocomposites. It is done to ensure that the nanocomposites have the combined excellent properties of both polymeric systems and their biodegradable nature, making their chains to break down easily and diffuse naturally back into the environment. (46) The addition of graphene nanofiller to the blend in various amounts will also be done to enhance the thermal and mechanical properties of the nanocomposites even further and incorporate the excellent characteristics of graphene nanoplatelets into the nanocomposites. (46, 48, 49) The aim of the study is to evaluate the optimum poly (lactic acid), polyurethane with cellulose acetate and graphene nanocomposite composition with the utmost superior properties required in various applications such as automotive areas, membrane technology, food packaging, etc. The study will also be extended to evaluate the underlying principles of the interaction of the chains of the two polymers with each other and with the nanofiller using advanced rubber-like elasticity theory, Flory-Erman constrained theory and Mark-Madkour trimodal network model.

2. Literature Review:

2.1. Nanocomposites:

Nanocomposites are materials composed of two or more materials, at which one of them at least has a dimension around 10^{-9} m, known as nanofiller. (50) These nanofillers are added to improve either the physical or the chemical properties of the obtained composite. The properties of the formulated nanocomposites depend on the morphological and interfacial features of the prepared composite in addition to the properties of the precursor from which the nanocomposites were prepared. Very minute amounts of nanofiller can dramatically affect the properties of the prepared matrix, due to the presence of very small inter-particulate distance between the particles of the nanofillers and due to the change in the morphological features of the nanocomposites which is due to the huge surface area to volume ratio of the particles compared to the macroscopic particles. (51)

Using nanofillers with polymers has various advantages; it will improve the thermal expansion and thermal conductivity of the polymeric matrix, as well as enhancing the mechanical properties as tensile strength, stiffness and toughness. Moreover, nanofillers can promote the gas and moisture barrier properties of different polymeric matrices. (52) Although nanofillers have several advantages, they also suffer from some limitations. They might limit the processability of nanocomposites due to the increase in viscosity. In addition to the uniform distribution hindrance that might occur due to the difficulty in the interfacial interaction and computability between the nanofiller and the matrix, which will finally cause nanofillers' agglomeration or sedimentation. (53, 54)

2.1.1. Poly(lactic acid)-based- Nanocomposites:

Composites having PLA blended with other natural polymers have been studied thoroughly through the last few years. Shumigin et al. studied composite resulting from blending the PLA with polyethylene and cellulose fibers using twin extruder. The effect of cellulose on the composite's properties was evaluated. It has been found that low amounts of cellulose have resulted in stiffer but more brittle materials. (55,56) Young's modulus increases and elongation at break slightly decrease. The composite was found

to improve the storage and loss moduli. The dynamic viscosity of the composite increases in the same manner as loss and storage moduli. (57)

Additionally, composites of PLA blended with PU were studied thoroughly. The blend was prepared by reactive processing and physical blending. The characterization of the blend has shown a successful coupling of the phases, which created more advantageous structure with higher mechanical properties. Moreover, the formation of submicron phases in the structure due to the large PU contents. Furthermore, natural poly butylene succinate (PBS) polymer was found to be successfully blended with PLA. (58) The composites were prepared with different compositions and examined their molded properties. Thermo-gravimetric analysis showed a higher thermal stability of the blends than pure PLA. The weight loss of the blend was lower than the neat polymers. DSC test indicated that thermal properties of PLA didn't change when blended with PBS. (59) Tensile strength and mechanical properties of blends decreased with the increase of PBS content in the blend. The impact strength of the blend was increased two folds compared to that of the pure PLA. (60) It was shown that addition of 10% and 20% of PBS increased the viscosity of the blend as well as storage modulus. An increase in the shear stress has been observed with the decrease of viscosity. (61) Finally, dynamic mechanical properties were investigated, observing a decrease in the storage modulus of all blends which indicates the increase of molecular mobility when PBS was added due to its lower glass transition. (62, 63, 64)

2.1.2. Polyurethane-based-Nanocomposites:

The dispersion of cellulose nano-crystals in polyurethane using solvent casting method was investigated. (65) It was observed an increase in the thermal degradation temperature while maintaining the stiffness, strength and elongation of the neat polyurethane. (66) A shift from 286 to 327°C in the glass transition temperature when 1 wt. % CNC was used. This shift was attributed to the formation of hydrogen bonds between the hydroxyl groups found on the surface of CNC and urethane groups found in the hard block. However, when 5 wt. % CNC was added, a minimal effect on the ultimate tensile strength and strain to failure was observed. (67)

Moreover, an extensive study was done on membrane prepared by blending polyurethane with cellulose acetate. It was found that the membrane contains common

structural groups as the initial materials as well as thermal stability up to 57°C. This study proved the suitability of the prepared blend membranes for wastewater treatment in textile industry. (68) The morphology of PU and its effect on its thermal and mechanical properties were explored. When hard segment crystallization was avoided by fast cooling, crystallization induced phase separation occurred upon reheating. At higher temperature, a second polymorph was additionally created. (69)

2.1.3. Cellulose acetate-based-Nanocomposites:

The blend of cellulose acetate with maleic anhydride grafted poly(lactic acid) was examined. This blend has shown superior mechanical properties as well as tensile strength due to the huge compatibility between the two components. (70) Well dispersion of cellulose acetate in the PLA-g-Ma matrix was achieved as a result of ester formation which occurred by creation of cross linked macromolecules between the carboxyl groups that are found in PLA-g-Ma and hydroxyl groups present in the cellulose acetate. (71)

Additionally, a blend of Cellulose acetate and polyethylene oxide copolymer was studied. The blend was prepared using γ -rays as initiator. Different concentrations of PEO additive in cellulose acetate were prepared. SEM has been used to explore the morphological changes. (72) Bulk properties as water sorption, electrical conductivity and chemical stability were all improved. Thermal stability was studied using TGA and DSC. The addition of small amounts of PEO (3 wt. %) resulted in a significant change in the thermal characteristics.

Cellulose acetate was proved to be environmentally friendly natural polymer, which encourage its use in different industrial applications. A study discussed that the use of biodegradable polymers provides an attractive solution to minimize environmental problems caused by the accumulation of waste plastics and landfills. (73)

PCL and CA were blended in different proportions with the addition of polyethylene-graft-glycidyl methacrylate as a compatibilizer. The addition of PE-g-GMA reduced the tensile strength as well as the elongation of the pure CA. However, the 20/80 blend increases the rigidity of the polymers. (74)

2.1.4. Natural polymers/ Carbon-based Nanocomposites:

The mechanical reinforcement resulted from the addition of carbon-based-nanomaterials such as graphene nanoplatelets (GnPs) and carbon nanotubes (CNTs) has been investigated. (75) Different GnPs' dimensions; 5 and 25 Mm, have been examined. It was observed that the bigger the flakes, the higher reinforcement as they control the mechanism of composite failure. (76) The use of CNTs with GnPs was also explored; it was found that by increasing the CNTs content, an improvement in the fracture toughness by 76% was obtained. However, the thermal conductivity increases with increasing the GnPs content in the polymeric matrix. (77)

2.1.4.1. Polypropylene/ Graphene Nanocomposites:

Nanocomposite resulting from blending exfoliated graphite nanoplatelets with polypropylene (PP) was prepared using a melt mixing procedure. TEM was used to check the uniform dispersion of the GnPs in the polymeric matrix. (78) It was found that all types of GnP were heterogeneous nucleation sites for PP crystallization. Moreover, the addition of GnPs enhanced the mechanical, heat resistance, thermal stability and conductivity of the blend compared to the plain PP. The increase in the thermal stability of the nanocomposites was due to the formation of flocculated thermal stable layer by the GnPs on the surface of the composite during the thermal degradation process. (79)

2.1.4.2. Polyurethane/Graphene Nanocomposites:

The homogenous dispersion of different types of graphene such as dispersible, functionalized, reduced, and graphene oxide-NH₂ were found to enhance the mechanical properties of PU. (80) An increase in the storage modulus as well as tensile strength and young's modulus was observed. In addition to the shape recovery, breaking stress and thermal properties; the modulus of the composite of 2wt% of graphene nanoplatelets was found to be ten times higher than pure PU sample, while it showed an increase by 7 times without losing elasticity when 4wt% of GP was used(81). Moreover, the stress transfer benefited from the interface between the PU and GP. An improvement in toughness of PU was also recorded after the addition of graphene. 50% improvement in toughness was achieved when 1wt% of GP without losing elasticity. (82)

Another study have shown that an improvement in the hardness and scratch resistance measured by nano indentation which was done with the incorporation of 4 wt of GO. A 6 C improvement was recorded in Tg of PU upon the addition of graphene nanofiller. Enhancement of thermal stability was also studied at 30 C with loading of 2wt of GP nanofiller compared to pure PU. (83)

2.1.4.3. Poly(lactic acid)/ Graphene Nanocomposites:

To overcome the shortcomings of PLA like the low heat deflection temperature of which impedes its industrial implementation for high performance applications. (84) Nanofillers were used to enhance the mechanical and thermal properties of PLA. The enhancement of the tensile properties of the nanocomposites is due to the orientation as well as the homogenous dispersion of the carbon based nanofiller in the polymer matrix and the strong interfacial interaction that occurs between the components, as well as their strong sp² carbon-carbon bonding and their geometric arrangement that enhances mechanical properties of the polymer matrix. (85)

A study demonstrated the design of PLA based nanocomposites using cellulose nanocrystals. It showed a higher storage modulus. While the use of graphene nanoplatelets xGnP as a nanofiller in PLA based blends, have shown an improvement in tensile modulus and elongation at break when low concentrations as 0.3wt% of xGnP was used. Moreover, plasticized nanocomposites have shown 100% higher yield in young's modulus than pure PLA. Moreover, it was found that the addition of a nanofiller to plasticized PLA will increase its tensile strength and elongation at break compared to plasticized PLA only; as nanofiller will act as both reinforcement filler and nucleating agent. On the other hand, it was found that using CNT-COOH nanofiller will give better results than using GnP as a nanofiller. As using GnP resulted in decrease in toughness and failure to reinforce the polymer matrix.

Thermal properties were also found to improve upon the addition of graphene nanofiller which was recorded using TGA; as it was recorded to increase with the increase of the xGnP nanofiller. Glass transition temperature showed maximum increase in PLA films with 5 C upon the addition of 0.4wt% GO and 7 C with Gnp nanofillers. (86)

2.1.4.4. Cellulose acetate/Graphene Nanocomposites:

Graphene based nanofillers were examined in many studies and showed an improvement in mechanical, thermal and thermo oxidative stability of cellulose acetate. It was found that the addition of GO nanofiller can provide homogenous composite films as well as being completely embedded within the CA matrix. (87) Exfoliated graphene and graphene nanoplatelets were also studied and found to be well dispersed and exfoliated in the matrix. Using 1wt% of exfoliated graphene was found to be the best concentration for it as nanofiller. Increasing the concentration of the nanofiller was found to cause aggregation in the composites. Enhanced dynamic mechanical modulus was also recorded upon the addition of higher concentrations of exfoliated graphene

Using graphene oxide as nanofiller with CA have shown better tensile properties which was widely used in UV shielding as it showed better UV shielding properties compared to pure CA. Thermal stability have shown an enhancement with the incorporation of graphene nanofillers with CA. Less weight loss with temperature was recorded with TGA to prove its effect on the thermal stability. Thermo oxidative stability of CA was also showed an enhancement with the addition of graphene nanofiller. Improved barrier properties against water vapor were recorded. The thermo oxidative stability of the composite under active oxygen improved, that is due to the gas barrier effect of graphene platelets that are dispersed in the matrix. SEM and XRD data showed that graphene platelets are well dispersed and exfoliated in the CA matrix for the composites. XRD measurements showed that the graphene oxide a uniformly dispersed. These nanocomposites can be further used in many electrical and electrochemical applications. (8)

3. Experimental:

3.1. Materials:

Poly (lactic acid) (PLA) pellets with a commercial name “Ingeo” grade 4043D of density 1.24 g/cc, relative solution viscosity (RV) of 4.0 (+/- 0.10), and D-Isomer level of 4.35% (+/-0.55%) was purchased from Nature Works LLC, Minnetonka, USA. Cellulose acetate (CA) powder with commercial name “cellulose acetate” of density 1.24 g/cc was purchased from Loba Chemie, India. Polyurethane (PU) pellets with commercial name “polyurethane” of density 1.21g/cc (± 0.02), eco-friendly and easy to process, was purchased from Honglu, China. All the polymers were used as received except for the PLA pellets; they were dried under vacuum at 40°C and 600 mbar for 5 hours. Carboxylic acid functionalized graphene nanoplatelets (GnPs-COOH) was purchased from Cheap tubes inc. Cambridge port, Vermont, USA. Finally, 1, 4- Dioxane (spectrophotometric grade ≥ 99 , Mwt. 88.11) was purchased from Sigma Aldrich.

3.2. Methods:

Different cellulose-acetate based composites have been prepared to improve its mechanical and thermal processability. Either Poly-lactic acid (PLA) or Polyurethane (PU) was added to form the composites. Additionally, both composites were prepared in both presence and absence of graphene nanoplateles (GnPs).

3.2.1. Preparation of Pure Polymers:

In order to investigate the enhancement in each blend pure polymeric films with 5 wt. % of CA, or PLA or PU in 1, 4-dioxane were first prepared using solvent casting method. Firstly, polymers were added to an Erlenmeyer flask with 1, 4 Dioxane extra pure solvent and allowed to stir for 8 hours at 60°C till complete dissolution. Then the polymeric solution was casted on a smooth, free of scratches glass plates using a laboratory-designed applicator. The initial thickness of the film was 0.7 mm. The cast films were kept in a closed environment to avoid formation of air bubbles or deformation of the films. The solvent evaporation extended for 24 hours at room temperature. Moreover, the glass plates were immersed in distilled water for 5-10 minutes to peel off the films. Finally, the films were dried under vacuum at 20°C and 600 mbar for 24 hours to eliminate any residual solvent.

3.2.2. Preparation of CA/PLA or CA/PU Composites:

The effect of PLA or PU on CA in the absence of GNPCOOH has been explored through preparing four ratios; 20%, 40%, 60% and 80% of CA of CA/PLA or CA/PU of total 5 wt% in 1, 4-dioxane using solvent casting method. Firstly, polymers were added to an Erlenmeyer flask with 1, 4 Dioxane extra pure solvent and allowed to stir for 8 hours

at 60°C till complete dissolution. Then the polymeric solution was casted on a smooth, free of scratches glass plates using a laboratory-designed applicator. The initial thickness of the film was 0.7 mm. The cast films were kept in a closed environment to avoid formation of air bubbles or deformation of the films. The solvent evaporation extended for 24 hours at room temperature. Moreover, the glass plates were immersed in distilled water for 5-10 minutes to peel off the films. Finally, the films were dried under vacuum at 20°C and 600 mbar for 24 hours to eliminate any residual solvent.

3.2.3. Preparation of GnPs-COOH-Based Nanocomposites

Three different GnPs-COOH-based nanocomposites, with CA, PLA and PU solely to observe the effect of GnPs on each polymer, were prepared using the same solvent casting method. Different concentrations of GnPs-COOH were tested 0.1 wt%, 0.3 wt%, 0.5 wt%, 0.7 wt% and 1 wt%. it was observed that the best results were obtained from 0.5wt% concentration. In each nanocomposite 0.5 wt. % of the GNPCOOH were added to form a total 5 wt. % polymeric solution in 1, 4-dioxane. 10 ml of 1, 4-dioxane was added to the 0.5 wt. % GnPs-COOH and sonicated using a Probe Sonicator for 2 minutes till uniform dispersion. The remaining solvent was added to the 4.5 wt. % polymer and left to stir for 8 hours at 60°C till complete dissolution. Then, the GnPs

solution was added to the polymeric solution and left to stir for 2 hours at RT. Then the polymeric solution was casted on a smooth, free of scratches glass plates using a laboratory-designed applicator. The initial thickness of the film was 0.7 mm. The cast films were kept in a closed environment to avoid formation of air bubbles or deformation of the films. The solvent evaporation extended for 24 hours at room temperature. Moreover, the glass plates were immersed in distilled water for 5-10 minutes to peel off the films. Finally, the films were dried under vacuum.

3.2.4. Preparation of CA/PLA or CA/PU withGnPs-COOH Nanocomposites:

Finally Nanocomposites of CA with GnPs-COOH in either the presence of PLA or PU were prepared using solvent casting method. In each nanocomposite 0.5 wt. % of the GnPs-COOH were added to form a total 5 wt. % polymeric solution in 1, 4-dioxane. These two Nanocomposites were prepared with 4 different CA wt % ratios namely, 20%, 40%, 60% and 80%. Firstly, 10 ml of 1, 4-dioxane was added to the 0.5 wt. % GnPs-COOH and sonicated using a Probe Sonicator for 2 minutes till uniform dispersion. The remaining solvent was added to the 4.5 wt. % polymer and left to stir for 8 hours at 60°C till complete dissolution. Then, the GnPs solution was added to the polymeric solution and left to stir for 2 hours at RT. Then the polymeric solution was casted on a smooth, free of scratches glass plates using a laboratory-designed applicator. The initial thickness of the film was 0.7 mm. The cast films were kept in a closed environment to avoid formation of air bubbles or deformation of the films. The solvent evaporation extended for 24 hours at room temperature. Moreover, the glass plates were immersed in distilled water for 5-10 minutes to peel off the films. Finally, the films were dried under vacuum at 20°C and 600 mbar for 24 hours to eliminate any residual solvent.

3.3. Characterization Techniques:

3.3.1. Fourier Transform Infra-Red Spectroscopy: (FT-IR)

Thermo-Scientific, Nicole 380 FT-IR at the Chemistry department, American University in Cairo (AUC) was used to reveal and confirm the chemical structures of the prepared samples, to report whether any new bonds of interactions were formed during blending or not. The films were cut into 2 cm x 2 cm with thickness of 0.7 mm. FTIR measurements were obtained by averaging 32 scans at resolution of 4 cm. FTIR spectra of pure powdered nanofiller were obtained by KBr pellet technique using the same instrument. All the prepared samples were analyzed in the wavelength range from 400-4000 cm^{-1} wavenumber.

3.3.2. Scanning Electron Microscopy: (SEM)

Scanning electron microscope instrument (Supra 5S LEQ, Zeiss) at 30kv shown in Figure (3.1) at the STRC, American University In Cairo, was employed to study the distribution of the nanofiller on the polymer's surface.

The scanning electron microscope images the surface of the sample by scanning it with a high energy beam of electrons. The technique of energy dispersive X-ray analysis is used to investigate the elemental composition of the sample which is found commonly on many scanning electron microscopes.

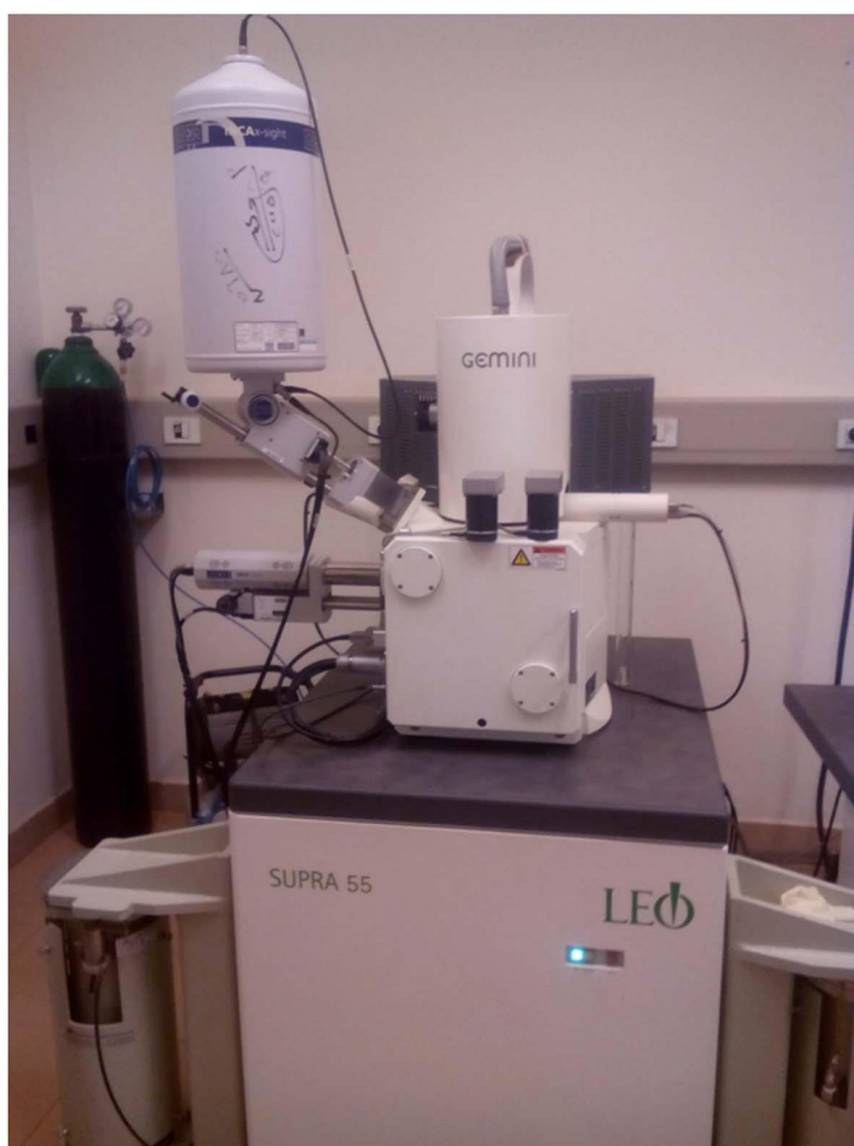


Figure 3.1 Scanning Elctron Microscopy

3.3.3. Thermogravimetric Analysis: (TGA)

The thermal stability profiles of the different samples were revealed using *Thermogravimetric Analysis (TGA Q50, TA Instruments)* shown in *Figure (3.3)* at the chemistry department, American University in Cairo. Each polymeric film were placed in the platinum pan and tested under a 60 ml/min purge of nitrogen. The samples were then heated up to 500°C at a rate of 10°C /min.



Figure 3.2 Thermogravimetric analysis instrument.

3.3.4. Differential Scanning Calorimetry: (DSC)

Differential Scanning Calorimetry instrument (perkinelmer PYRSIS diamond autosampler, Waltham, Massachusetts USA) shown in *Figure (3.2)* at the STRC, American University in Cairo was employed to assess the thermal behavior of the prepared composites and the effect of nanofiller on the thermal behavior of the nanocomposites. The investigated films were cut into small pieces with weight of around 17 mg of each sample and placed in a 50 mL aluminum pan and sealed with a cover using universal crimper press. Heating-cooling-heating cycles were performed under nitrogen atmosphere. During the experiment, samples were heated from 0°C to 180°C at rate of 10°C/min, and held at 180°C for 10 minutes. The samples were then cooled from 180°C to 0°C at rate of 10°C/min and held at 0°C for 10 minutes. This process was repeated one more time.



Figure 3.3 Differential Scanning Calorimetry instrument

3.3.5. Stress/Strain Measurements:

Isomers of stress-strain of all samples were done at room temperature. Samples were obtained from casted films specimens. Samples free of air bubbles and pinholes that possess specific width, length and thickness of 1.5 cm x 9 cm x 0.0085 cm respectively were cut from CA/PLA, CA/PU, CA/PLA/GnP_s-COOH and CA/PU/GnP_s-COOH to evaluate the mechanical response of the sample and influence of the addition of the nanofillers to the blend and its mechanical behavior according to the equation

$$[f^*] = f/[A^* (\alpha - \alpha^2)]$$

Where $[f^*]$ is the modulus, A^* is the cross-sectional area and α is the elongation.

The equilibrium elastic force F^* was recorded after the force reading has become constant for at least 10 minutes.

3.3.6. Dry Thermal Degradation Test:

In order to test for the degradability of the developed bio-nanocomposites, the oven method will be used in accordance with *ASTM 0573-99*. Specimens for degradation will be placed in an air oven preheated to 100 °C. The specimens will be subjected to the thermal degradation treatment for 14 days. After degradation, the specimens will be removed from the oven, cooled to room temperature on a flat surface and allowed to stand for not less than 24 hours prior to further testing.

4. Results and Discussion:

The aim behind preparing different nanocomposites through blending diverse natural biodegradable polymers with graphene nanoplatelets (GnPs) as nanofiller is to enhance the poor thermal and mechanical properties and to produce cost effective, environmentally friendly materials to be used in various applications. The polymers used in preparing those novel nanocomposites are poly (lactic acid), polyester-based polyurethane and cellulose acetate. Those polymers have been chosen to guarantee that the nanocomposites will possess their biodegradable nature leading to the easy breakdown of the polymeric chains and their natural diffusion back into the environment. Different Techniques were employed to investigate the structural, physical and chemical properties of the prepared nanocomposites such as FTIR, SEM, TGA, Stress/Strain measurements and dry thermal degradation tests.

4.1. Investigation of the molecular interaction of the Prepared Nanocomposites:

Fourier Transform Infrared Spectroscopy (FTIR) was used to ensure the successful preparation of the targeted nanocomposites in addition to the examination of the molecular interaction force resulted from the blending in order to get a better understating of the molecular behavior.

4.1.1. Fourier Transform Infrared Analysis: (FT-IR)

As shown in *Figures (4.1-4.7)* pure polymers and polymeric blends are compared to those mixed with the nanofiller (GnPs) to ensure their blending and investigate the type of interaction. Successful blending of CA with GnPs-COOH is demonstrated in *Figure 4.1*, it was observed that the neat CA has two characteristic peaks; broad peak O-H stretching at 3485 cm^{-1} characteristic to hydroxyl group and sharp peak C=O stretching at 1731 cm^{-1} characteristic to carbonyl group. GnPs used in the nanocomposites were functionalized with carboxylic groups. As the nanofiller was introduced to the CA, a slight shifting in the carbonyl peak from 1731 cm^{-1} to 1734 cm^{-1} was observed, indicating the hydrogen bonding interactions between CA matrix and GNPS-COOH. No additional functional groups have been observed in the FT-IR

spectrum which proves that the only interaction occurred was the hydrogen bonding between the carbonyl group of the CA with the carboxylic group of the GnPs-COOH.

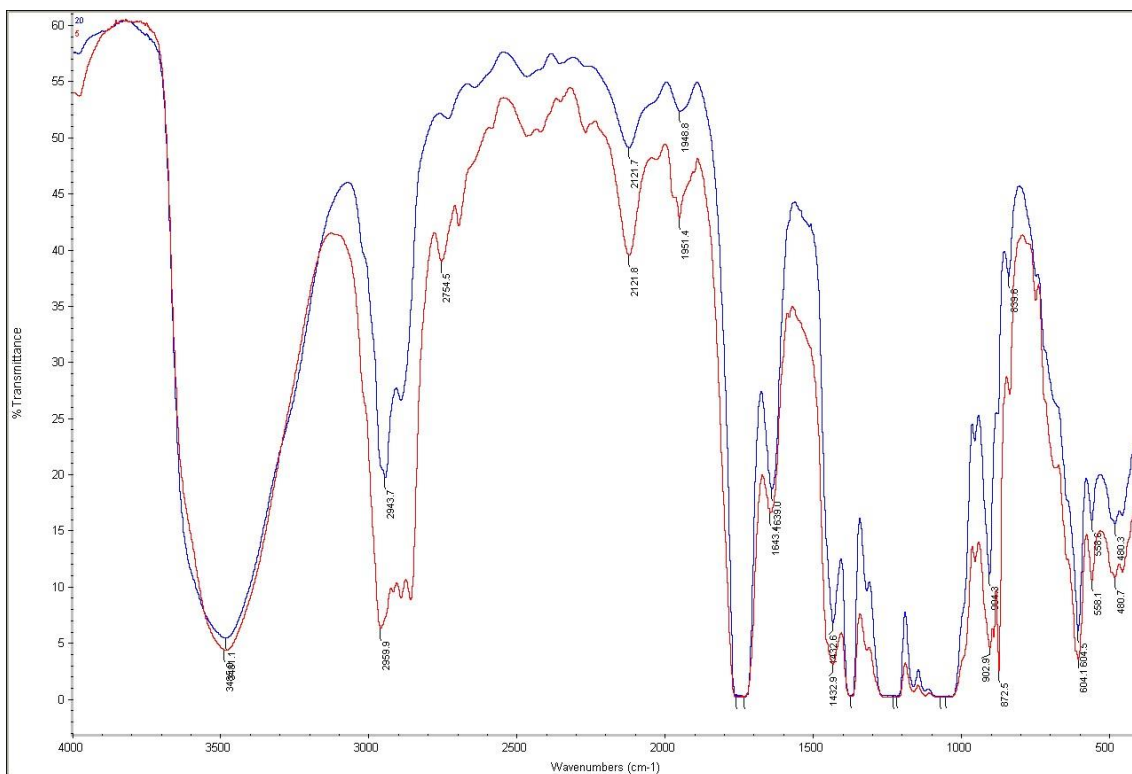


Figure 4.1 FT-IR spectra of — neat CA in comparison with the — CA/GnPs-COOH nanocomposite.

FTIR spectra of neat PLA in comparison with the PLA/GnPs-COOH nanocomposite are shown in **Figure 4.2**. It was observed that the neat PLA has three characteristic groups; two sharp medium peaks O-H stretching at 3503 and 3600 cm^{-1} characteristic to the hydroxyl and carboxylic groups, and sharp peak C=O stretching at 1751 cm^{-1} characteristic to carbonyl group. When the GnPs-COOH nanofiller was introduced to the PLA a slight shifting from 1751 to 1782 cm^{-1} in the carbonyl group peak, indicating the hydrogen bonding interaction occurred between the C=O of the PLA and the COOH of the nanofiller. Moreover, no additional functional groups have been observed in the nanocomposite indicating the absence of any other type of interactions.

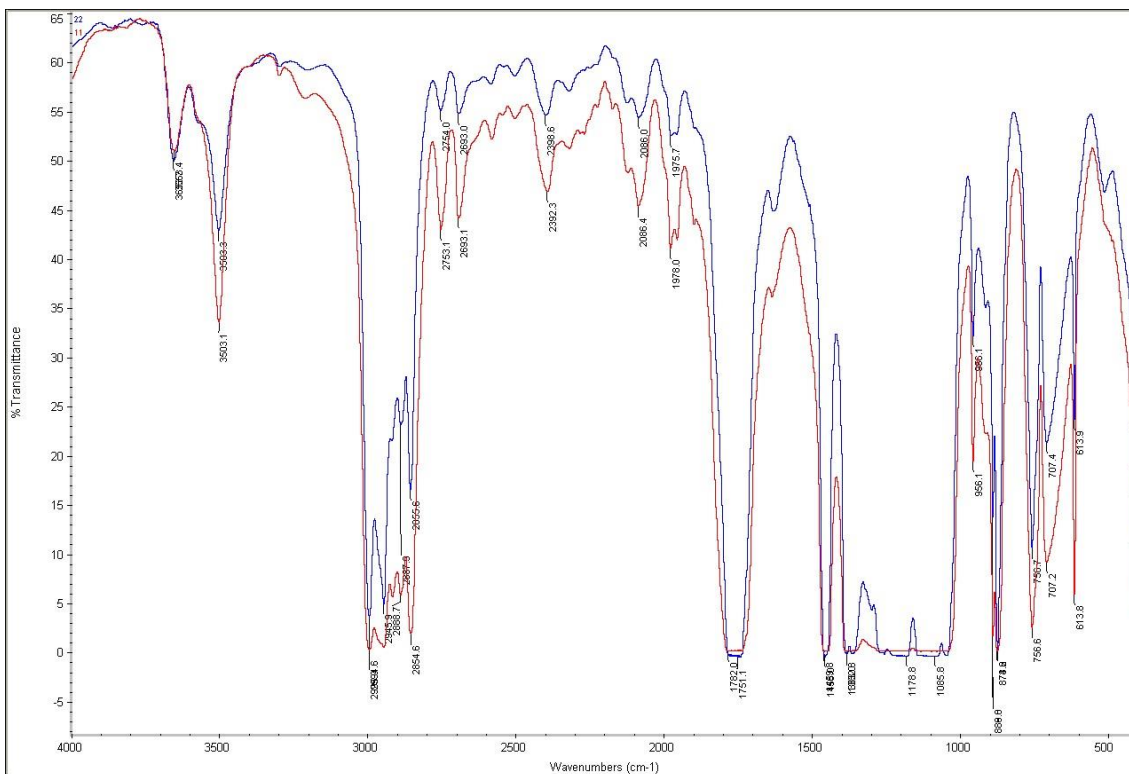


Figure 4.2 FT-IR spectra of — neat PLA in comparison with — PLA/GnPs-COOH nanocomposite.

FT-IR spectra for neat PU in comparison with PU/GnPs-COOH nanocomposite are shown in **Figure 4.3**. It is observed that the PU has three characteristic peaks; sharp peaks N-H stretching at 3334 cm^{-1} , C=O stretching at 1701 cm^{-1} characteristic to the amide group and C-C aliphatic at 2958 cm^{-1} characteristic to the methyl group. When the functionalized GnPs were introduced to the PU a slight shifting in the C-C peak from 2958 to 2981 cm^{-1} and the N-H peak was also shifted and broadened at 3541 cm^{-1} .

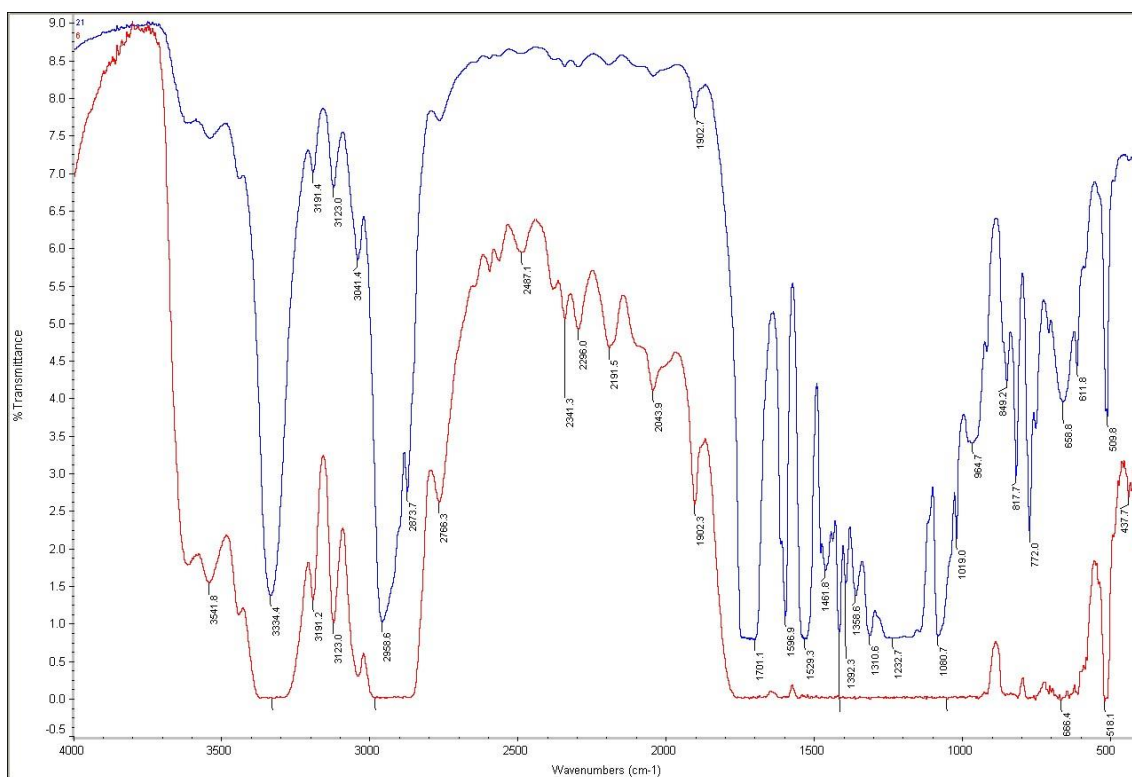


Figure 4.3 FT-IR spectra of —neat PU in comparison with the — PU/GnPs-COOH nanocomposite.

FT-IR spectra of PLA/CA in comparison with PLA/CA/GnPs-COOH nanocomposite are shown in **Figures 4.4 and 4.5**. After comparing the blend with the nanocomposite, it was observed that all the characteristic peaks of the PLA, CA and their nanocomposites with GnPs-COOH; C=O stretching at 1734 cm^{-1} and O-H stretching at 3503 cm^{-1} were merged. Although different ratios between the PLA and CA were prepared, same results were observed.

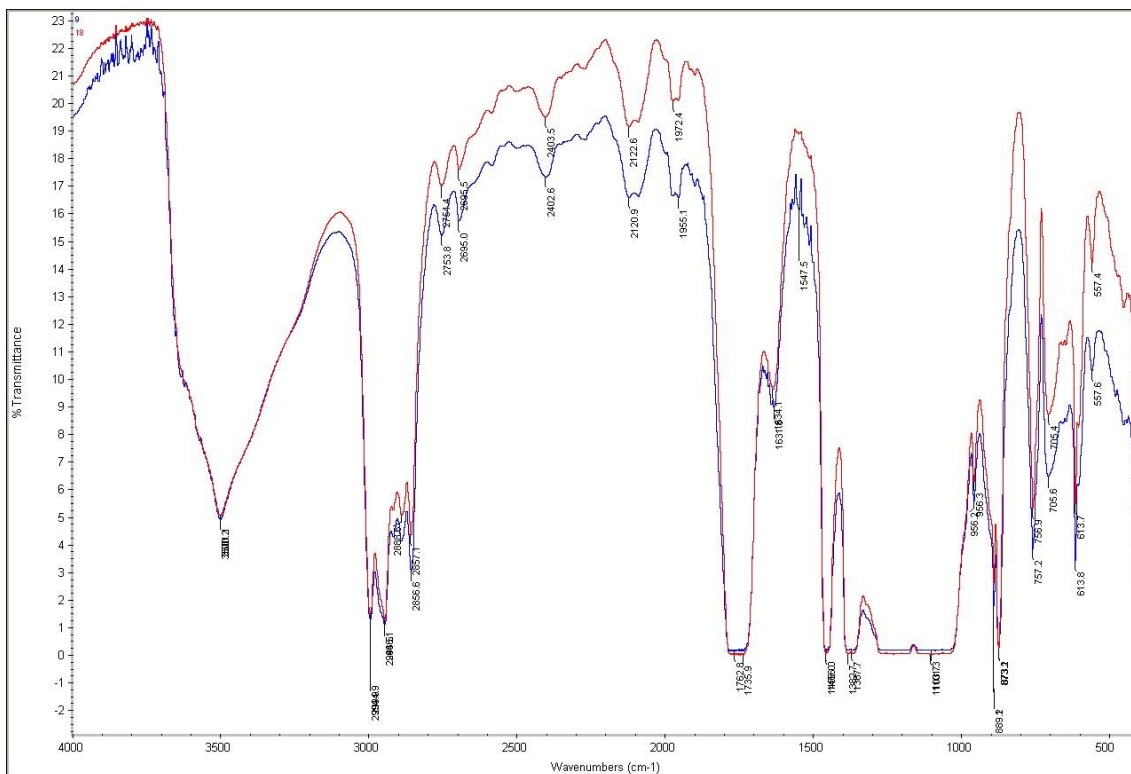


Figure 4.4 FT-IR spectra of — 60% PLA/CA in comparison with — PLA/CA/GnPs-COOH Nanocomposite.

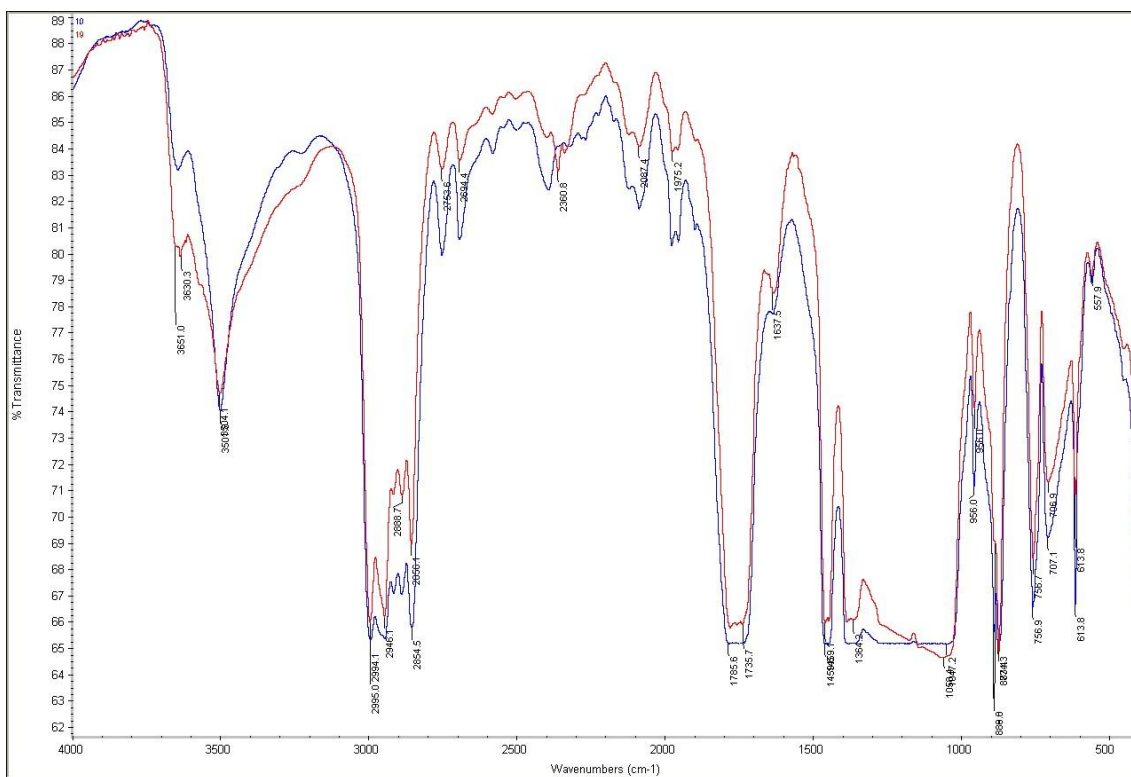


Figure 4.5 FT-IR spectra of — 80% PLA/CA in comparison with — PLA/CA/GnPs-COOH Nanocomposite.

FT-IR spectra of PU/CA in comparison with PU/CA/GnPs-COOH nanocomposite are shown in **Figures 4.6 and 4.7**. After comparing the blend with the nanocomposite, it was observed that all the characteristic peaks of the PU, CA and their nanocomposites with GnPs-COOH; N-H stretching at 3541 cm^{-1} and C-C stretching at 2981 cm^{-1} were merged. Although different ratios between the PU and CA were prepared, same results were observed.

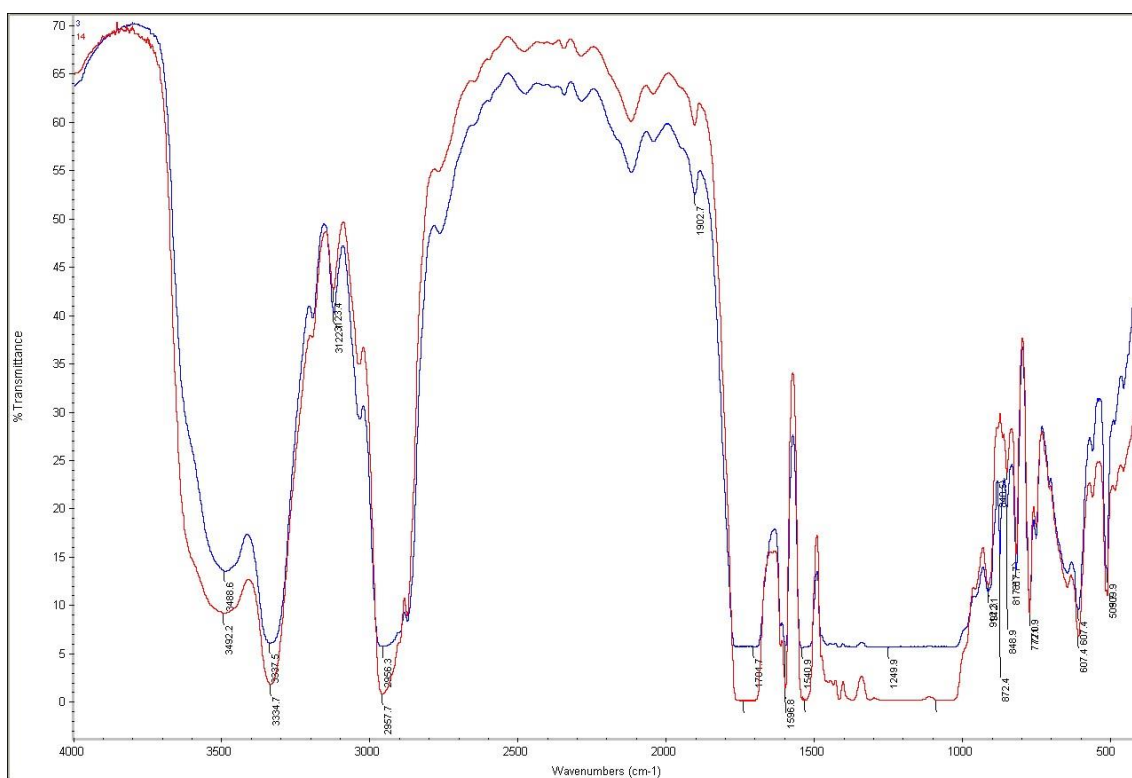


Figure 4.6 FT-IR spectra of — 60% PU/CA in comparison with
— PU/CA/GnPs-COOH Nanocomposite.

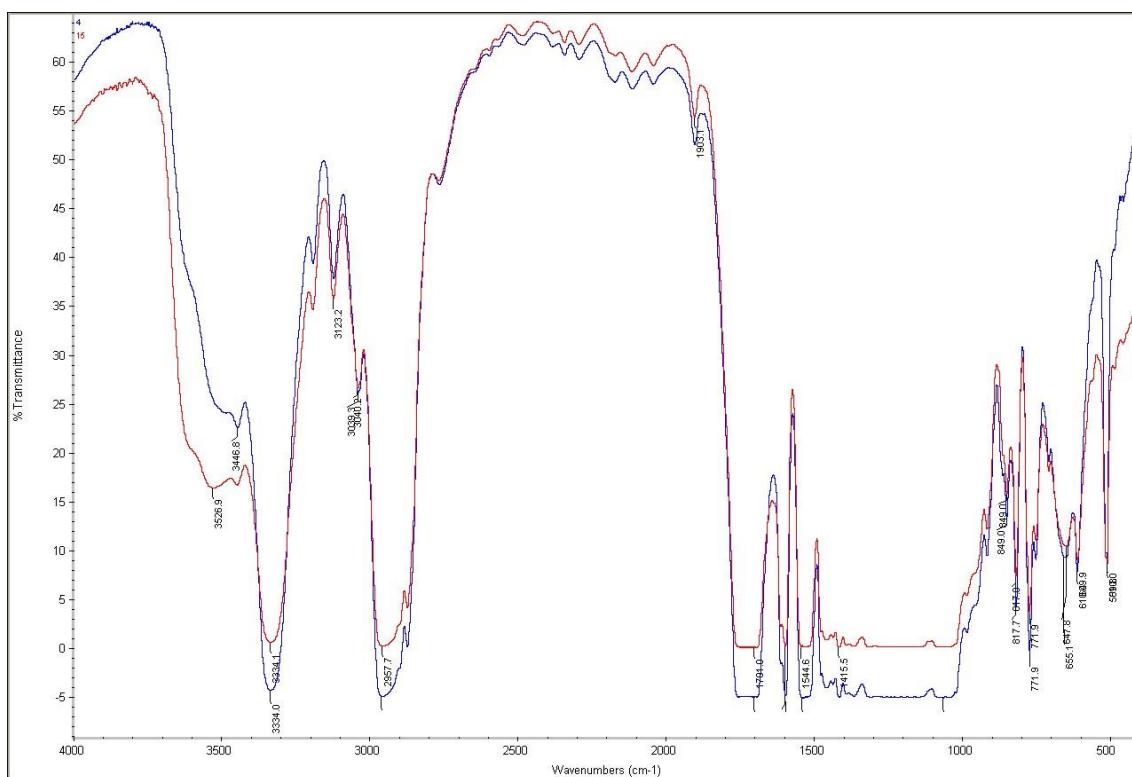


Figure 4.7 FT-IR spectra of — 80%PU/CA in comparison with PU/CA/GnPs-COOH Nanocomposite.

4.2. Investigation of the nanofiller dispersion throughout the polymeric matrices of the prepared nanocomposites:

Uniform dispersion of the GnPs throughout the various polymeric matrices prepared in the different nanocomposites was explored using scanning electron microscopy.

4.2.1. Scanning Electron Microscopy Analysis: (SEM)

Figures (4.8-4.14) show the micrographs of PLA/GnPs-COOH, PU/GnPs-COOH, CA/GnPs-COOH, PLA/CA/GnPs-COOH and PU/CA/GnPs-COOH respectively. It was observed that graphene nanoplatelets flakes were evenly distributed in the different matrices, which proves its complete blending within the polymeric chains without forming any agglomerations. This might be due the hydrogen bonding interaction occurred with different polymers present in the different nanocomposites prepared. Hydrogen bonding maintained the uniform dispersion through fixing the nanofiller in its position. Uniform dispersion will validate any results obtained from the mechanical testing that will be proposed further in this chapter.

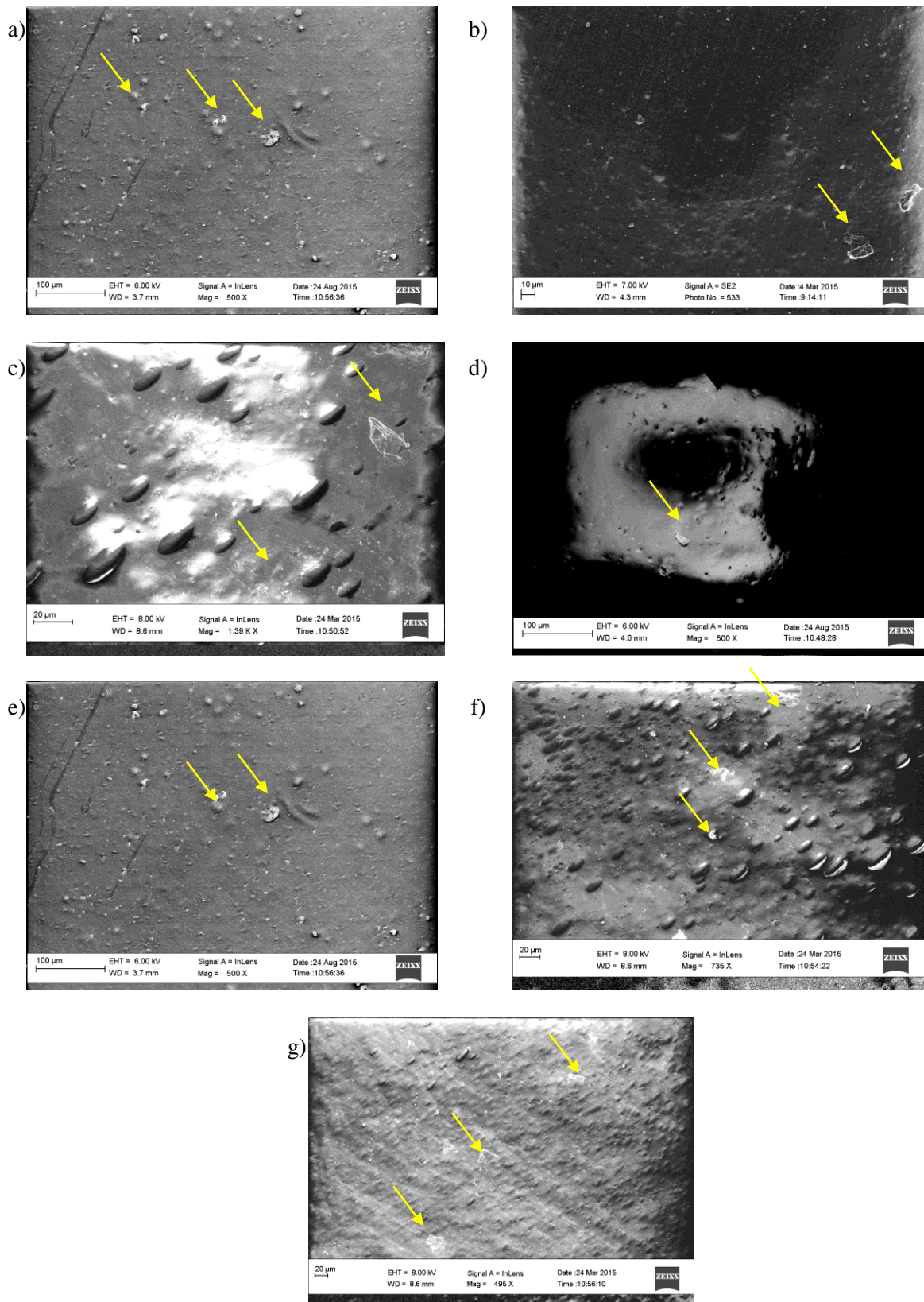


Figure 4.8 SEM micrographs of a) CA/GnPs-COOH, b) PLA/GnPs-COOH, c) PU/GnPs-COOH, d), e) PLA/CA/GnPs-COOH and f), g) PU/CA/GnPs-COOH

4.3. Investigation of the Thermal Properties of the Prepared Nanocomposites:

As mentioned previously, one of this work targets is to enhance the thermal stability of the produced nanocomposites. Therefore, thermogravimetric analyzer was used to evaluate the thermal stability of the prepared nanocomposites upon addition of GnPs-COOH nanofiller.

4.3.1. Thermogravimetric Analysis: (TGA)

TGA thermograms of CA, PLA and PU with 0.5% wt GNPS-COOH nanofiller in comparison with their neat are depicted in **Figures (4.9-4.11)**. The diagrams showed an improvement in thermal stability of the nanocomposites after the addition of the nanofiller. It revealed that the initial decomposition temperature (T_{onset}) and the decomposition temperature at 50% weight loss ($T_{50\%}$) for CA, PLA and PU nanocomposites have increased compared to neat CA, PLA and PU as shown in **Table 4.1**

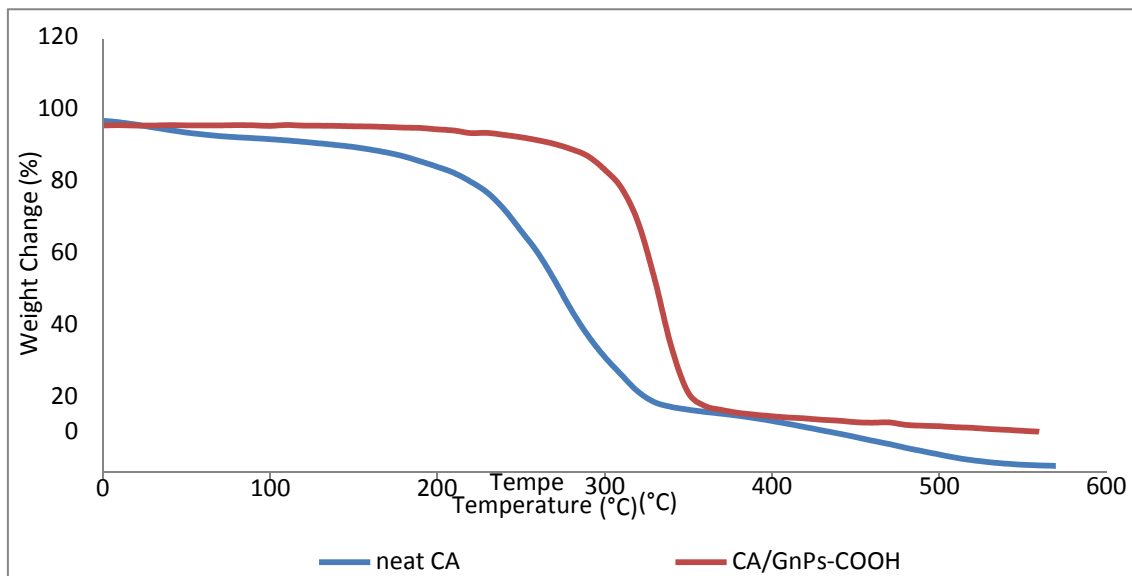


Figure 4.9 TGA thermograms of neat CA in comparison to CA/GnPs-COOH

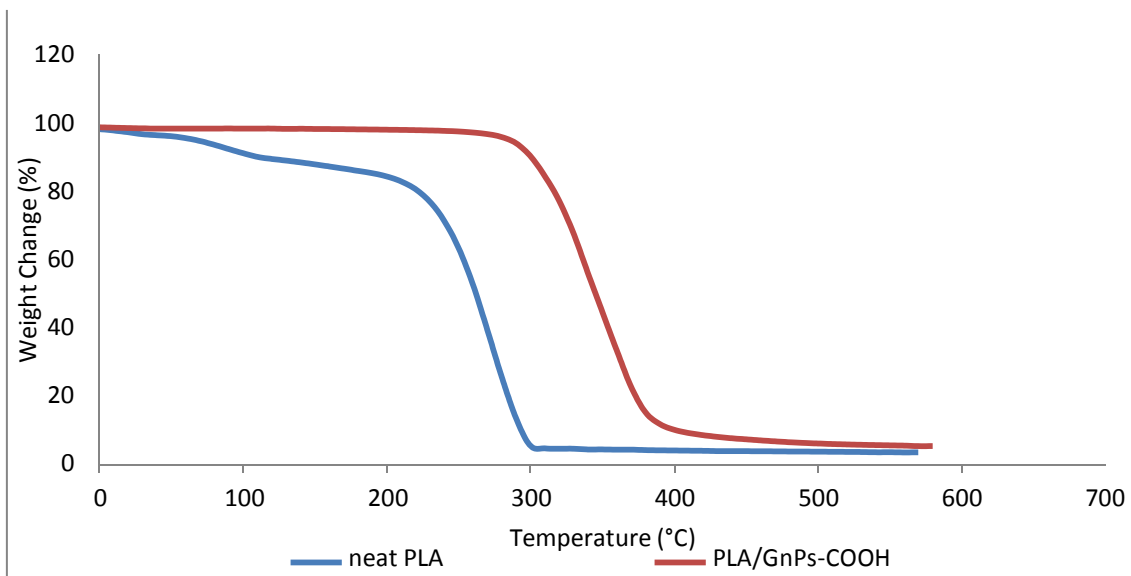


Figure 4.10 TGA thermograms of neat PLA in comparison to PLA/GnPc-COOH

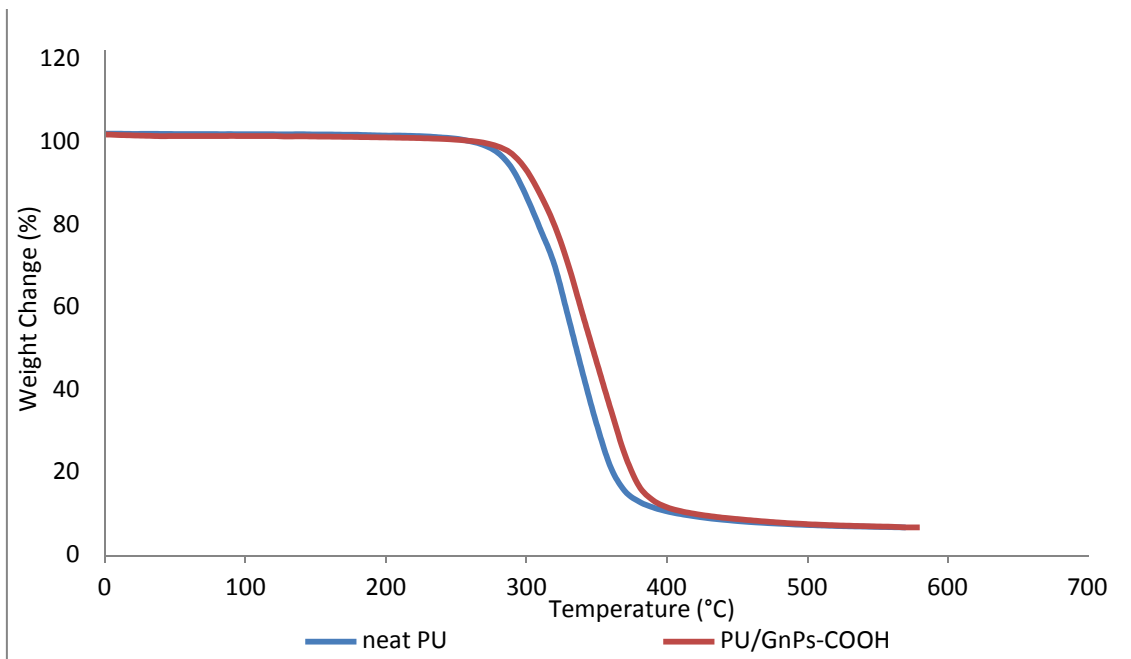


Figure 4.11 TGA thermograms of neat PU in comparison to PU/GnPc-COOH

Table 4.1 neat CA,PLA and PU in comparison to CA, PLA and PU nanocomposites

Material	T _{onset} (°C)	T _{50%} (°C)	T _{max} (°C)
Neat CA	209.8	300.3	360
Neat PLA	220.5	290.4	320
Neat PU	290.1	360.5	390
CA/GnPs-COOH	280.7	370.4	360
PLA/GnPs-COOH	280.5	360.6	390
PU/GnPs-COOH	299.8	381.2	400

PLA/CA/GnPs-COOH nanocomposites TGA thermograms in comparison with PLA/GnPs-COOH and CA/GnPs-COOH are shown in **Figure 4.12**. Among those nanocomposites the PLA/GnPs-COOH showed the highest thermal stability, however, CA/GnPs-COOH showed the lowest stability. By adding PLA to CA/GnPs-COOH, the thermal stability increased. Moreover, the higher the PLA ratio, the higher the thermal stability, and the higher the degradation temperature were observed as shown in **Table 4.2**.

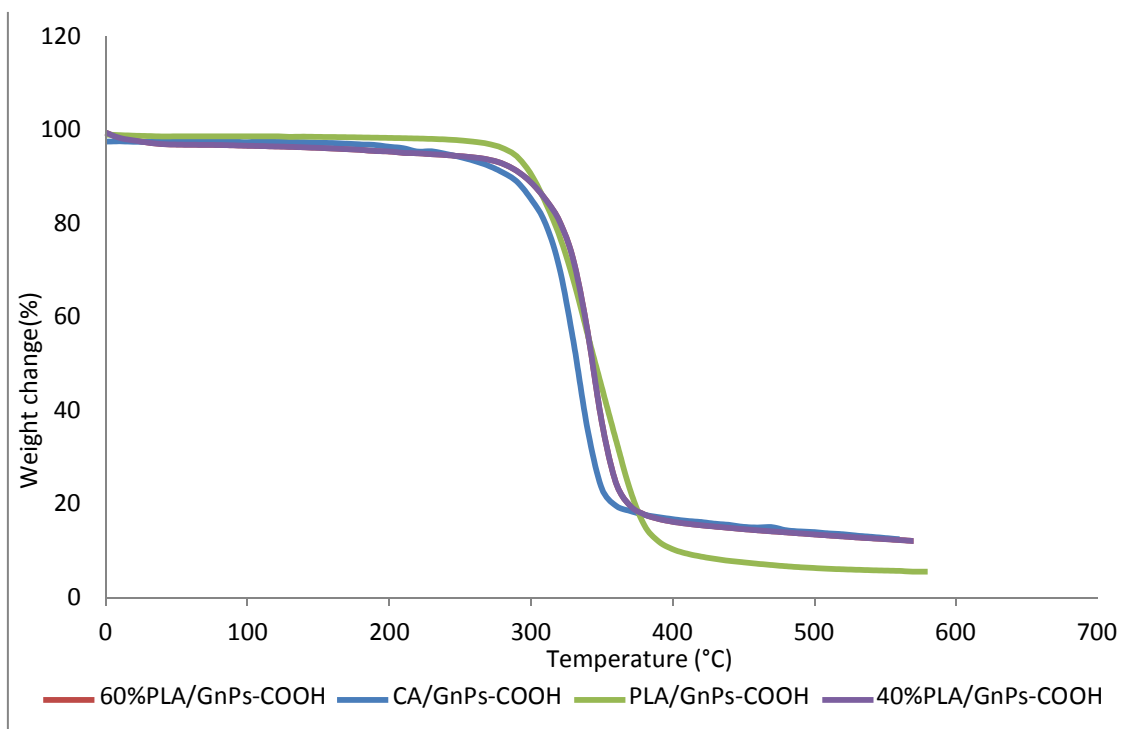


Figure 4.12 TGA thermograms of PLA/CA/GnP-COOH nanocomposite in comparison with PLA/GnP-COOH and CA/GnP-COOH

Table 4.2 Characteristic temperatures at different ratios of PLA/CA/0.5wt% GnP-COOH

Material	T _{onset} (°C)	T _{50%} (°C)	T _{max} (°C)
Neat CA	209.8	300.3	360
20%PLA	229.5	289.7	330
40%PLA	229.8	290.1	330
60%PLA	230.45	290.4	330
80%PLA	230.6	290.5	330
Neat PLA	220.56	290.4	320
CA/GnP-COOH	280.7	370.4	360
20/PLA/GnP-COOH	289.2	369.7	360
40%PLA/GnP-COOH	290.2	370.1	360
60%PLA/GnP-COOH	290.54	370.4	360
80%PLA/GnP-COOH	290.65	370.5	360
PLA/GnP-COOH	280.54	360.6	390

PU/CA/GnPs-COOH nanocomposites TGA thermograms in comparison with PU/GnPs-COOH and CA/GnPs-COOH are shown in **Figure 4.13**. Among those nanocomposites the PU/GnPs-COOH showed the highest thermal stability, however, CA/GnPs-COOH showed the lowest stability. By adding PU to CA/GnPs-COOH, the thermal stability increased, as PU is known to be thermo-stable polymer. However, increasing the ratio of the PU, the degradation temperature did not change as shown in **Table 4.3**.

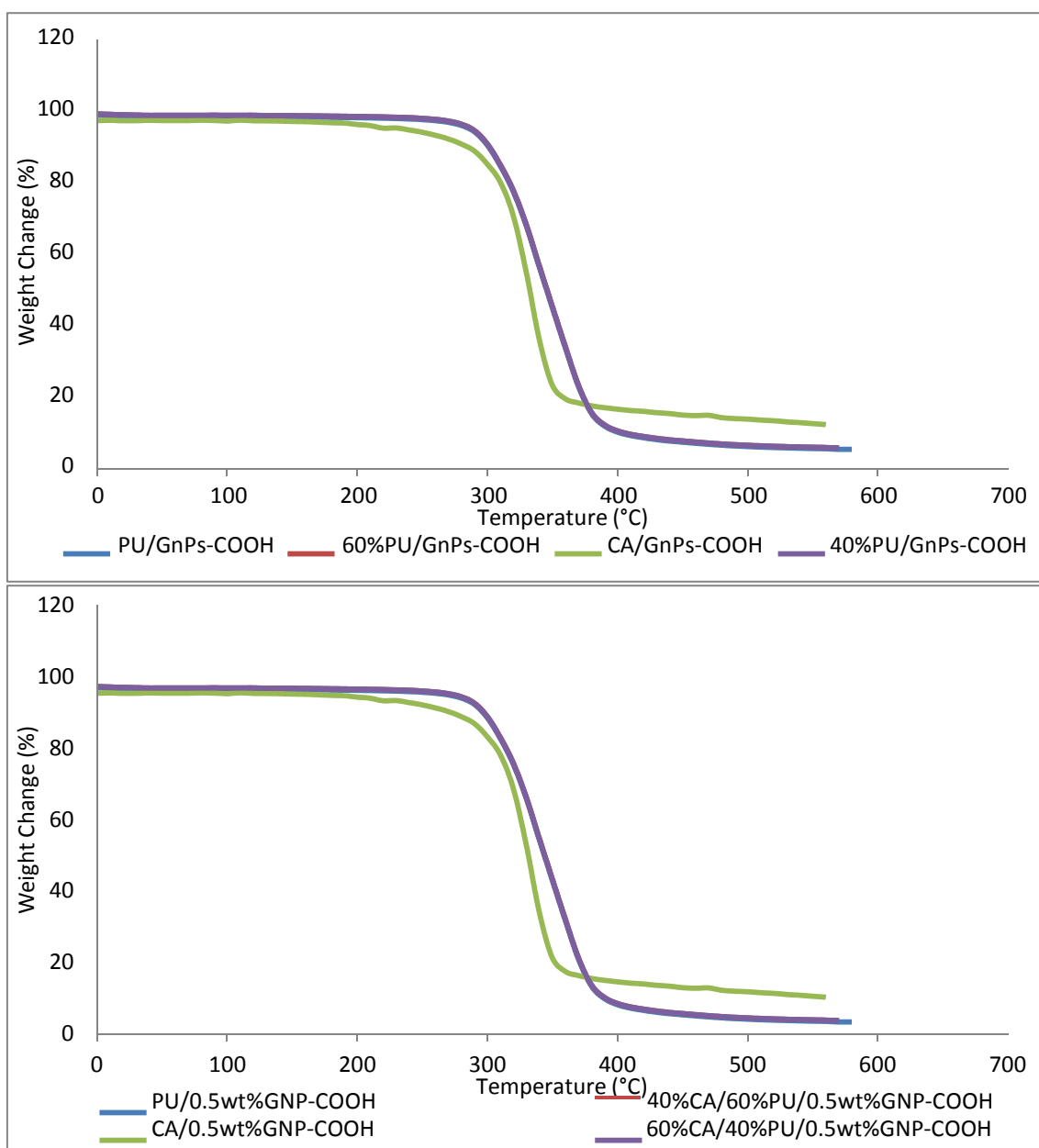


Figure 4.13 TGA thermogram of PU/CA/GnPs-COOH

Table 4.3 Characteristic temperatures at different ratios of PU/CA/GnPs-COOH

Material	T _{onset} (°C)	T _{50%} (°C)	T _{max} (°C)
CA/GnPs-COOH	280.7	370.4	360
20%PU/GnPs-COOH	309.6	375.1	400
40%PU/GnPs-COOH	309.8	375.4	400
60%PU/GnPs-COOH	310.4	375.6	400
80%PU/GnPs-COOH	310.9	375.7	400
PU/GnPs-COOH	299.8	381.2	400

As previously observed, CA polymer showed the lowest thermal stability and the PU showed the highest stability, therefore by adding PU to CA an improvement in the stability was observed more than that with adding the PLA. However, the addition of the nanofiller increased the degradation temperature in all cases. These results can be explained as functionalized GnPs possesses a high thermal stability that tends to degrade at 600°C. Moreover due to the high aspect ratio and lamellar structure of GnPs, this system may form a charred layer which prevents the permeation of oxygen. This layer formed an insulating surface that prevented the escape of gaseous molecules during thermal decomposition.

4.3.2. Differential Scanning Calorimetry analysis of CA, PLA, PU, PLA/CA and PU/CA with GnPs-COOH

The thermal behavior of CA/GnPs-COOH, PLA/GnPs-COOH, PU/GnPs-COOH, PLA/CA/GnPs-COOH, PU/CA/GnPs-COOH nanocomposites were tested using DSC as shown in *Figures (4.14-4.18)*. In general, it was observed that no peaks were recorded as the nanocomposites are said to be amorphous. This behavior can be explained as that glass transition temperature is a point where the amplitude of segmental oscillations of macromolecules rapidly changes. By increasing temperature, it only increases the frequency of the chains segments so no peaks are recorded

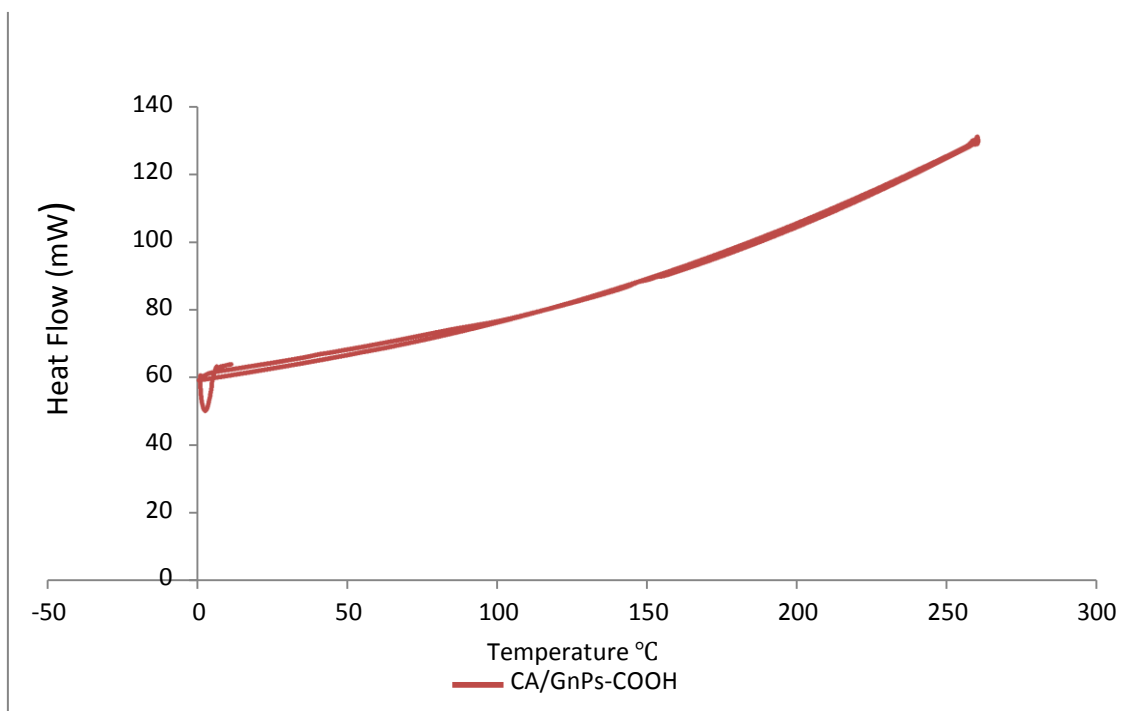


Figure 4.14 DSC thermogram for CA/GnPs-COOH

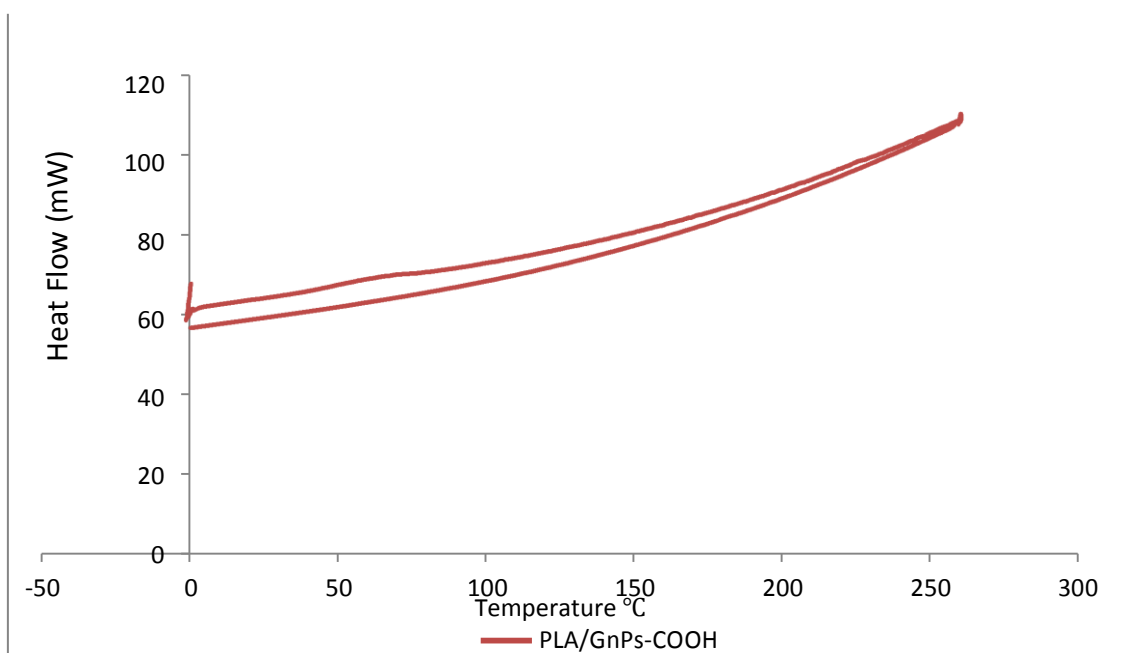


Figure 4.15 DSC thermogram for PLA/GnPs-COOH

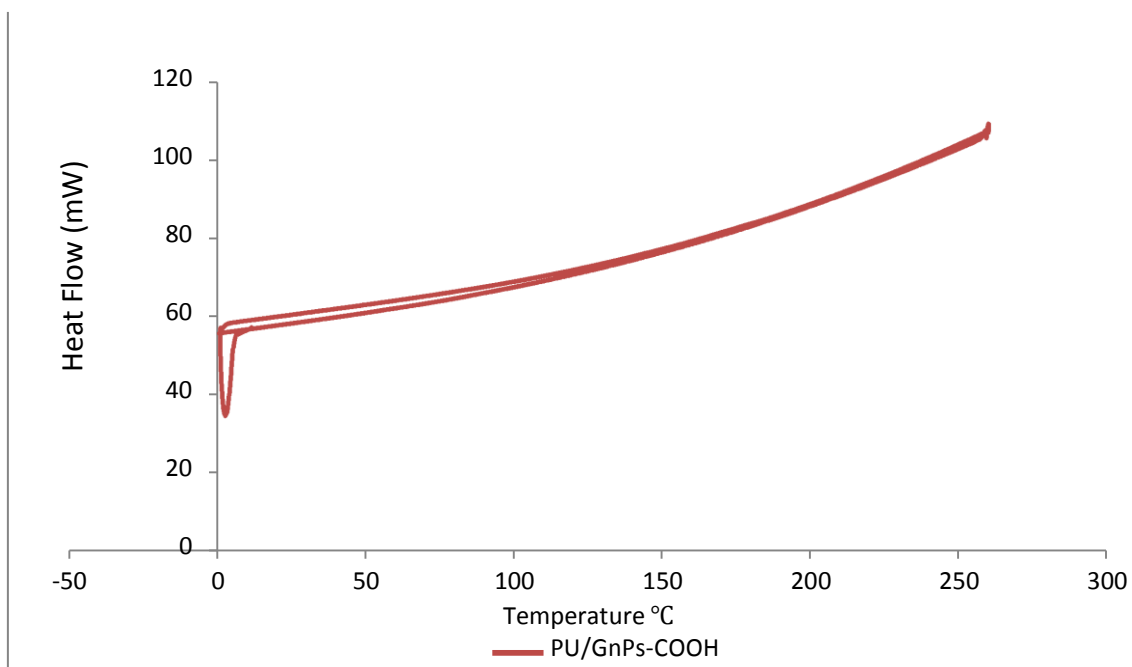


Figure 4.16 DSC thermogram for PU/GnPps-COOH

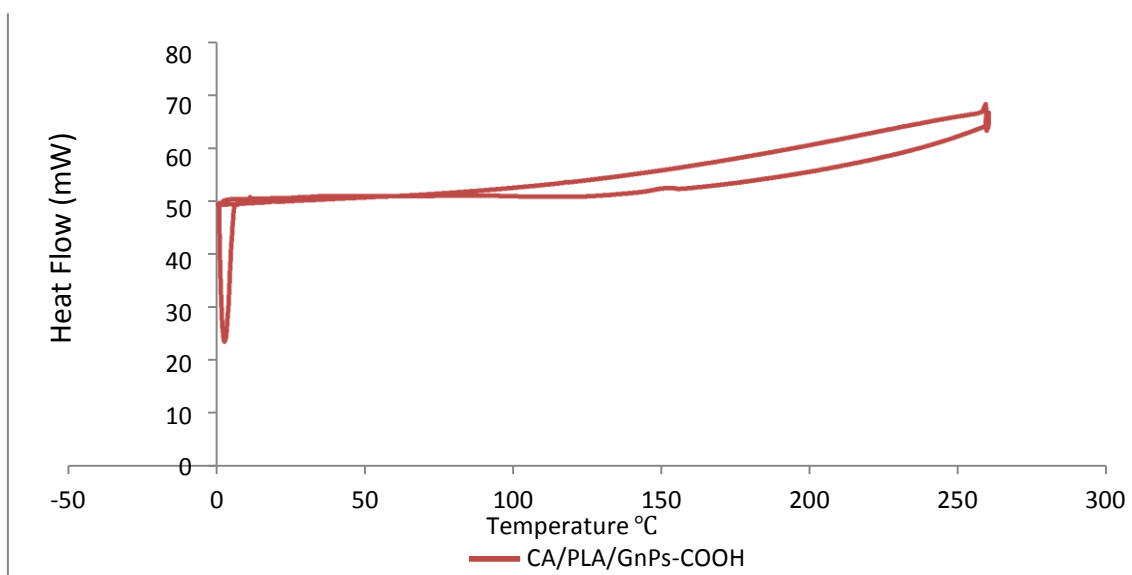


Figure 4.17 DSC thermogram for PLA/CA/GnPps-COOH

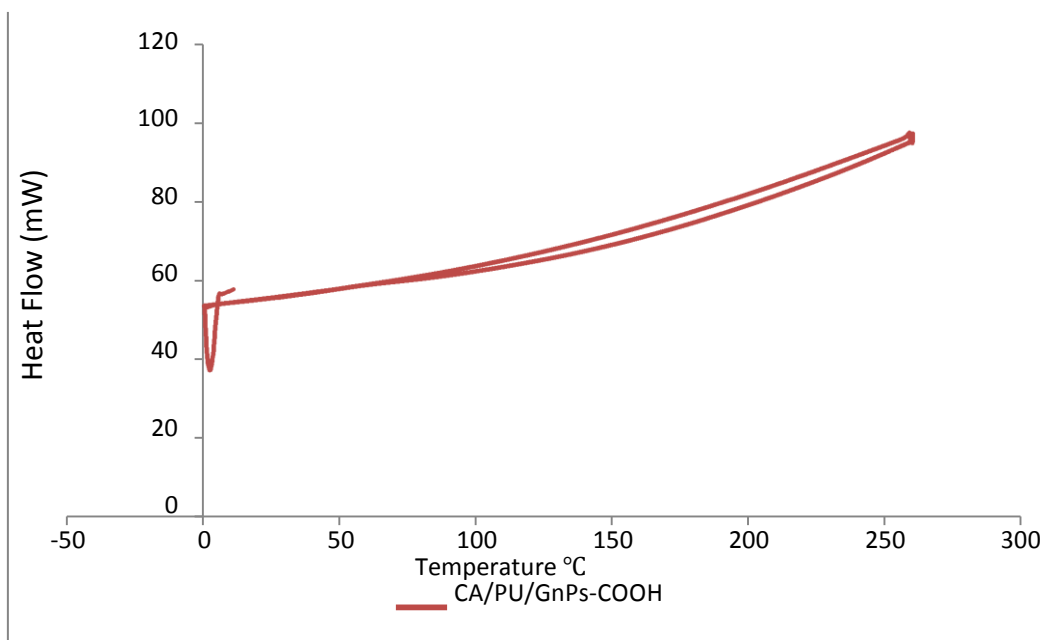


Figure 4.18 DSC thermogram for PU/CA/GnPc-COOH

4.4. Investigation of the Mechanical Properties of the Prepared Nanocomposites:

As mentioned previously, improvement of mechanical properties of the obtained nanocomposites is one of the objectives behind this work. Therefore, stress/strain measurements and dry thermal degradation tests were carried out to investigate the obtained mechanical properties and evaluate the enhancement.

4.4.1. Stress/ Strain Measurements:

These measurements are done to calculate nominal force, elongation at break and energy required to break the sample as mentioned previously in chapter three.

4.4.1.1. Neat CA, PLA and PU:

Mechanical properties based on single measurement for neat CA, PLA and PU were evaluated. CA showed moderate elastic modulus and very low elongation at break, which generally restricts its application in different fields, while PLA was observed to have moderate elastic modulus and low elongation at break. However, PU showed low elastic modulus and high elongation at break. Stress strain isotherms of neat CA, PLA and PU are represented in *Figures (4.19-4.21)*. Ultimate mechanical properties such as maximum nominal force (f^*_m), maximum elongation (α_m) and the maximum energy required to reach maximum nominal stress at maximum elongation (E_m) were calculated and reported in *Table (4.4)*.

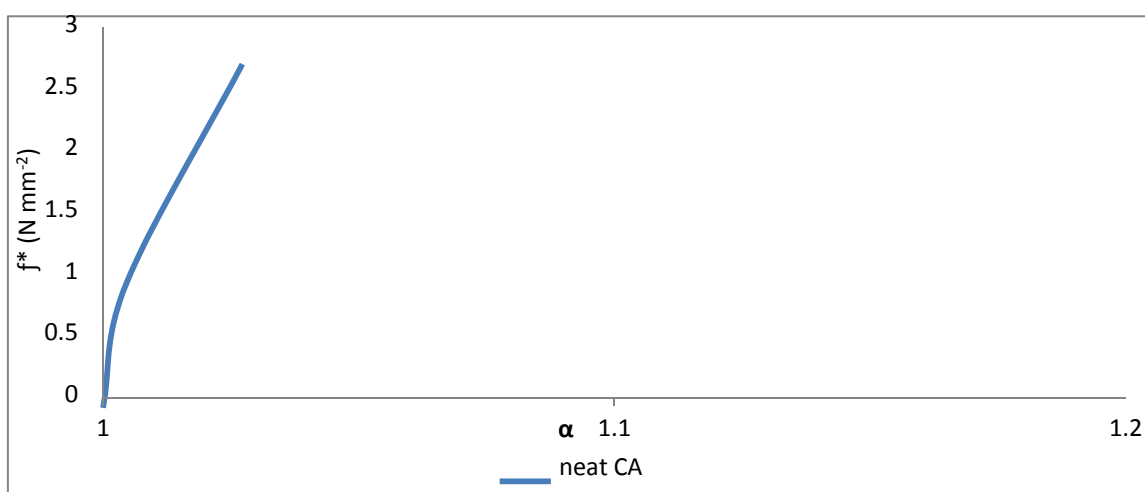


Figure 4.19 Stress-strain isotherm of neat CA.

As shown in *Figure 4.19*, CA exhibited high modulus and very low tensile elongation. This behavior was attributed to the rigid nature of cellulose backbone which restricts its inelasticity and low mobility due to the presence of massive 3D hydrogen bonding network between the various hydroxyl groups present alongside the polymeric backbone on CA.

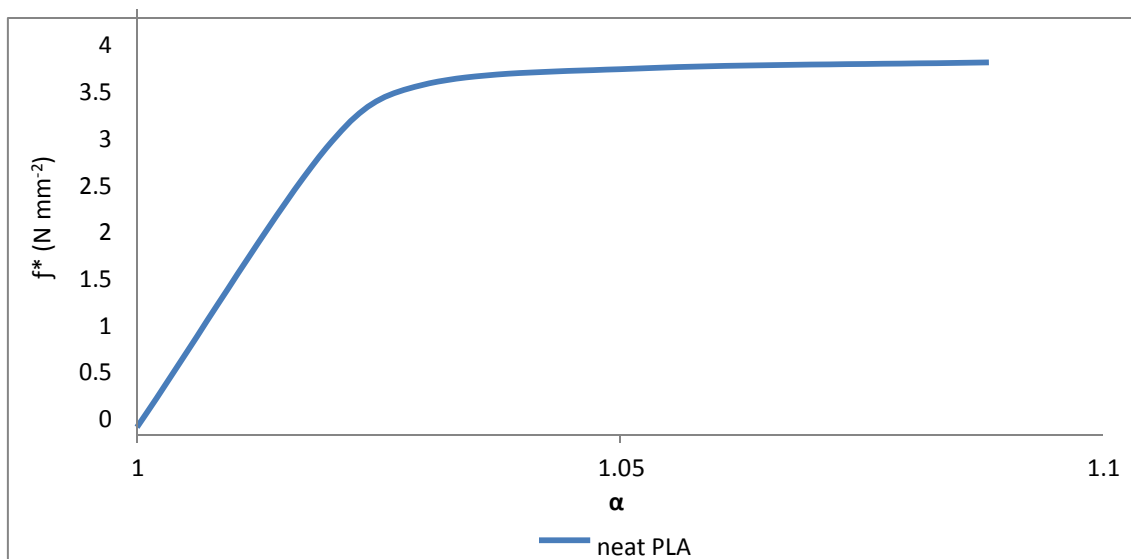


Figure 4.20 Stress-strain isotherm of neat PLA.

In *Figure 4.20* it was shown; however, that PLA exhibited high modulus and very low tensile elongation. This behavior attributed to the rigid behavior of PLA and low mobility that restrict its use when it's below its glass transition temperature T_g . This behavior was attributed to the high glass transition of PLA (about 63°C) as shown by using DSC analysis. Below this T_g , PLA exhibits rigid behavior and low mobility that restrict its application.

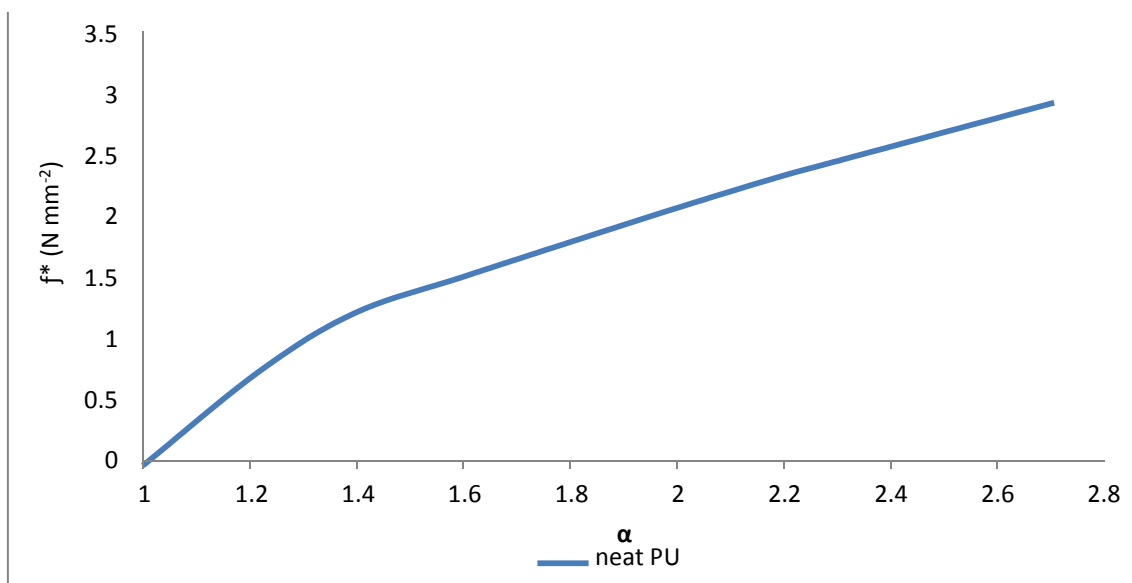


Figure 4.21 Stress-strain isotherm of neat PU.

Figure 4.21, shown however that PU exhibited high tensile elongation and modulus which makes it an excellent candidate for various applications. This excellent mechanical properties possessed by PU is due to its segmented nature where the hard blocks act as filler particles connecting the elastic soft blocks.

In order to overcome the shortcomings in the mechanical performance of the various polymers such as low elongation at break, for PLA and CA and high hysteresis for PU, blends of different polymer combinations with different compositions were prepared and investigated.

4.4.1.2. PLA/CA Composites:

It was suggested that the addition of PLA to CA may affect the mechanical behavior of the blend. In that regards, different ratios of PLA were added to CA. Namely, 20, 40, 60 and 80 PLA wt. % were used. Mechanical properties of the four ratios were tested and represented in **Figure 4.22**.

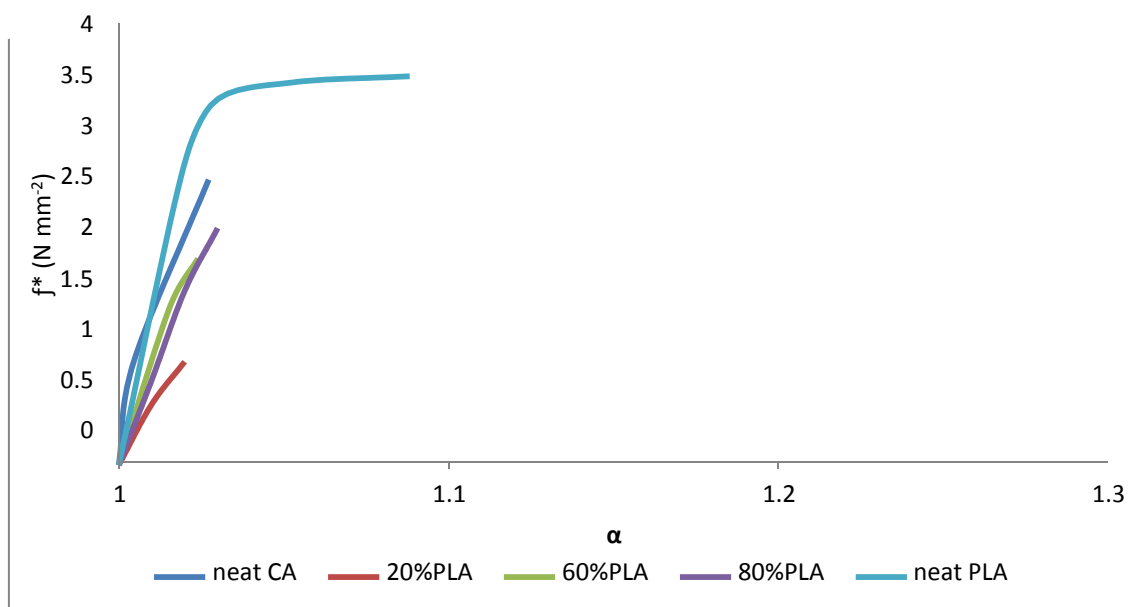


Figure 4.22 Stress-Strain isotherm of PLA/CA composites at different ratios.

Uniform dispersion of all components and effective wetting in a given matrix are important factors. Interfacial adhesion between the two phases is required in order to get a composite with good mechanical integrity. As can be seen from the figure above, CA showed poor interfacial adhesion with PLA in the matrix. This poor interfacial adhesion in the matrix is due to hydrogen bonds formation between CA as well as the disparate hydrophilicities of PLA and CA. Tensile strength at break decreased continuously and markedly as the CA content increased. This might be due to the poor dispersion of CA in the matrix of PLA which significantly affects the mechanical properties of the composite. **Table 4.4** depicts the ultimate mechanical properties for CA/PLA blends at different ratios of PLA.

Table 4.4 Ultimate mechanical properties for neat CA and PLA/CA composite at different ratios.

Material	α_m	f_m^* (N mm ⁻²)	E_m (J mm ⁻³)	Hardness
Neat CA (0%PLA)	1.03	2.7	0.22	18
20% PLA	1.02	1.007	0.0185	9
60% PLA	1.024	2.01	0.02	11
80% PLA	1.03	2.31	0.18	14
Neat PLA (0%CA)	1.08	3.79	1.7	20

From the table, it was observed that the tensile elongation slightly increased with the increase of the concentration of PLA in the matrix. Maximum nominal force showed a decrease with the increase in the concentration of CA. The energy required to break the sample showed a significant decrease at both concentration of 20%, 60% of PLA. This is probably due to the increased stiffness of the material of the composite arising from the different hydrophilicities of the materials which hindered the efficient wet mixing. Hardness of the examined material showed a decrease consistent with the other decrease in the corresponding mechanical properties of the CA/PLA composite.

4.4.1.3. PU/CA Composites:

It was suggested that the addition of PU to CA may enhance its mechanical properties. Thus, in these regards different ratios of PU were added by weight to CA. Namely, 20%, 40%, 60% and 80% PU were used. Investigating the effect of different ratios of PU to CA blend on the mechanical properties of the blend is represented in *Figure 4.23*.

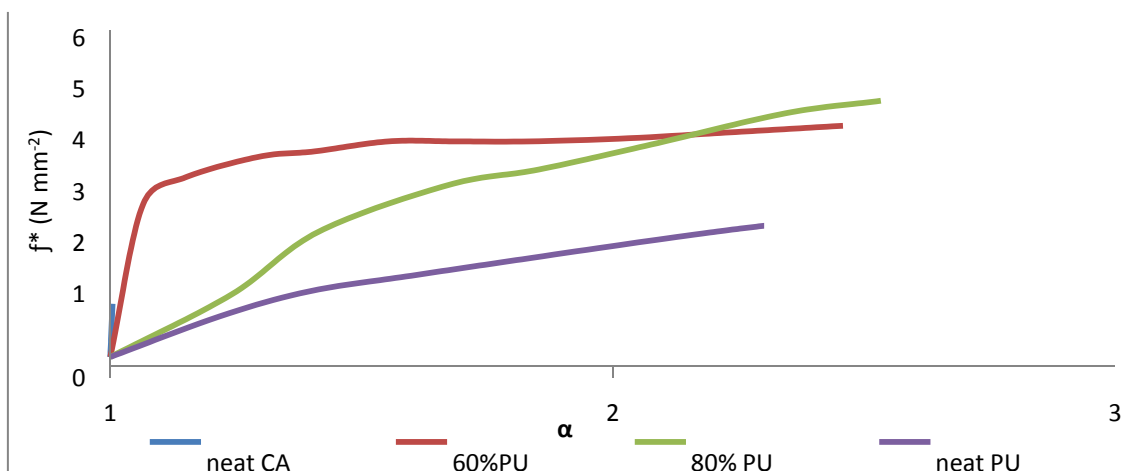


Figure 4.23 Stress-Strain isotherm of PU/CA composite at different ratios.

Complete dispersion of PU in CA matrix occurred, which resulted in well mixed blend. At low concentrations of PU, 20% and 40%, samples failed to be tested for their mechanical properties as they have maximum elongation instantly. Tensile strength at break decreased continuously and markedly as the CA content increased. Polar groups in the hard segments have decreased the mobility of chains which decreased its tensile strength in turn. Upon the addition of higher ratio of PU at 60% and 80% of PU, mechanical properties of the blend showed a significant increase compared to neat CA and PU. This can be due to the full molecular interaction between the PU and CA. **Table 4.5** depicts the ultimate mechanical properties for CA/PU blends at different ratios of PU.

Table 4.5 Ultimate mechanical properties for PU/CA composites.

Material	A_m	f_m^* ($N\ mm^{-2}$)	E_m ($J\ mm^{-3}$)	Hardness
Neat CA (0%PU)	1.02	2.7	0.22	19
60%PU	2.4	4.3	4.68	31
80%PU	2.5	4.8	5.1	34
Neat PU (100%PU)	2.3	3.6	3.7	38

From the table, it was observed that the tensile elongation increased with the increase of the ratios of PU in the matrix, at 60% and 80% PU showed the highest increase in maximum elongation. Maximum nominal force showed a significant increase with the increase in the ratios of PLA, 60% and 80% PLA showed the highest increase. The energy required to break the sample showed a significant and highest increase at high ratios of PU. At 60% and 80% of PU. This indicates the increased toughness of the material. These findings shows that composite of CA and PU blend possess very good mechanical properties.

4.4.1.4. PLA/CA/GnPs-COOH Nanocomposites:

In order to improve the mechanical properties of the polymers and to study the nanofiller's effect on the mechanical behavior of the composite, nanofiller of functionalized graphene nanoplatelets (GnPs-COOH) was added at the concentration of 0.5 wt%. Nanofiller particles help the blending process of the polymeric chains on the molecular level as different chains will get adsorbed on the surface of the nanoplatelets forcing them to molecularly mix. This approach is used to overcome their limitations by increasing their deformability and flexibility. The nanofiller used in this study was chosen based on its ability to improve the polymers response to stress, low content used, its compatibility and low toxicity.

Blending the biopolymers of PLA/CA with 0.5wt% functionalized graphene nanoplatets may improve the mechanical properties of the composite. In this regards, 0.5wt% GNPS-COOH was added to different ratios of PLA/CA composites prepared. *Figure 4.24* shows the stress-strain curves for the nanocomposites at different ratios of PLA/CA.

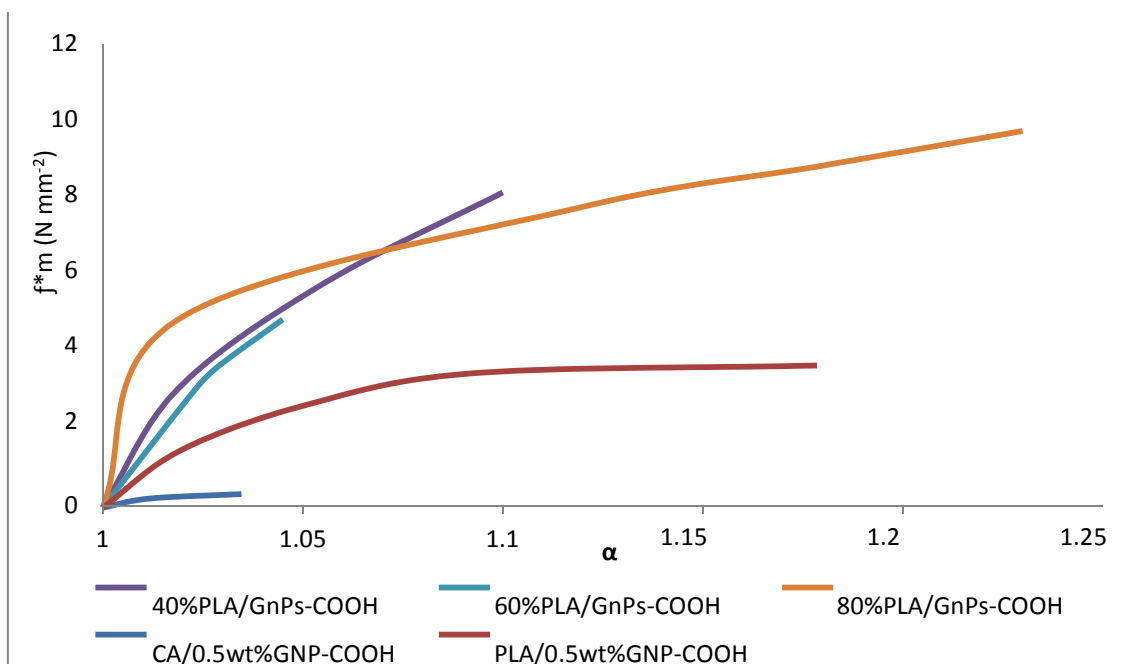


Figure 4.24 Stress-strain isotherms of PLA/CA/GnPs-COOH nanocomposites.

It was observed that the nominal force as well as the elongation at break; have increased. GNPS-COOH lamellar or flake like structure enhanced the exfoliation of the nanofiller and thus, helped in the dispersion of the nanofiller within the matrices of the composite. Hydrogen bonding was formed between the carbonyl group of PLA, hydroxyl groups of PLA with the carboxylic groups of GnPs-COOH. **Table 4.6** compares between the maximum elongation (α_m), maximum nominal force (f^*m), and amount of energy required to break the sample or reach maximum point (E_m) for different ratios of CA/PLA/GnPs-COOH nanocomposites and CA/PLA blends.

Table 4.7 Ultimate mechanical properties for CA/PLA/GnPs-COOH nanocomposites and CA/PLA blends at different ratios

Material	α_m	f^*m (N mm ⁻²)	E_m (J mm ⁻³)	Hardness
CA/ GnPs-COOH	1.03	0.3	0.207	19
20%PLA/ GnPs-OOH	1.045	4.9	0.13	20
60%PLA/GnPs-COOH	1.1	8.2	0.52	11
80%PLA/GnPs-COOH	1.23	9.8	2.09	30
PLA/ GnPs-COOH	1.17	3.7	1.28	22

According to the data presented in the table, incorporating GnPs-COOH into the matrices of CA/PU has shown a total increase in the mechanical properties of the blend. Maximum elongation showed an increase by 0.9%, 6.8% and 19.4% at ratios of 20%PLA, 60%PLA and 80%PLA respectively. Tensile elongation at break showed an increase for ratios 20%, 60% and 80% PLA/0.5wt%GnPs-COOH. The energy required to break the material shown an increase for ratios 60% and 80%PLA/0.5wt%GnPs-COOH. This increase in energy is attributed to the increased toughness of the material; which is done by the incorporation of GnPs-COOH to the material induced flexibility to PLA matrix, induced by the motion of the molecular chains to resist the applied stress.

4.4.1.5. PU/CA/GnPs-COOH:

A constant concentration of the nanofiller, Functionalized Graphene Nanoplatelets 0.5wt%, was added to the different ratios of CA/PU composite in order to study its effect of its mechanical properties. **Figure 4.25** show the stress - strain curves for the nanocomposites of different ratios of CA/PU/ GnPs-COOH

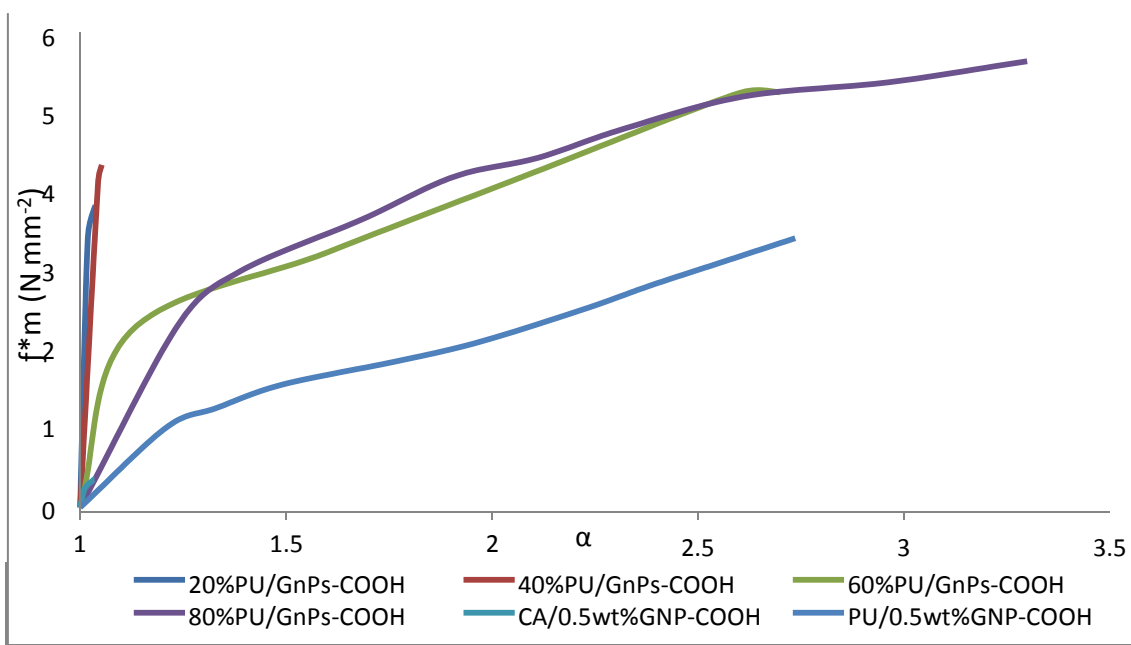


Figure 4.25 Stress-Strain isotherm of PU/CA/GnP-COOH nanocomposites.

It was observed that the nominal force increased as well as the elongation at break. GnP-COOH lamellar or flake like structure enhanced the exfoliation of the nanofiller and thus, helped in the dispersion of the nanofiller within the matrices of the blend. The nano effect relies on the interfacial area between the matrix and the filler which is significantly augmented in a nanocomposite compared to bulk matrix. This can be due to the extensive hydrogen bonding formed between the carboxylic groups of the nanofillers and the carbonyl ester group of polymeric chains thus enhancing the dispersion of the nanofiller in the matrix. Improved mechanical properties of the nanocomposite can be also due to the transfer of the stress from the matrix to the nanofiller which enhance the properties of the nanocomposite. **Table 4.7** compares between the maximum elongation (α_m), maximum nominal force (f^*m), amount of energy required to break the sample or reach maximum point (E_m) and hardness for different ratios of CA/PU/GnP-COOH nanocomposites.

Table 4.7 Ultimate mechanical properties for PU/CA/GnPs-COOH nanocomposites.

Material	α_m	f_m^* (N mm ⁻²)	E_m (J mm ⁻³)	Hardness
CA/ GnPs-COOH	1.03	0.35	0.2	20
20%PU/GnPs-COOH	1.04	3.8	0.27	21
40%PU/ GnPs-COOH	1.05	4.3	0.38	38
60%PU/ GnPs-COOH	2.7	5.1	6.4	40
80%PU/ GnPs-COOH	3.3	5.6	9.5	40
PU/ GnPs-COOH	2.9	3.6	4.67	40

According to the data presented in the table, incorporating GnPs-COOH into the blend of CA/PU has shown an increase in the mechanical properties of the blend. Tensile elongation showed an increase at all concentration of the CA/PU nanocomposite with maximum increase by 162% and 220% at ratios 60% and 80%PU/GnPs-COOH. Maximum nominal force has shown also a significant increase upon the incorporation of the nanofiller to the composite. Highest increase at ratios of 80% and 60%PU/GnPs-COOH. It was also observed that the energy required to break the material have shown a significant increase at ratios of 60% PU and 80% PU/0.5wt%GnPs-COOH respectively. These results were ascribed to the increased toughness of the composite.

4.5.2. Dry Thermal Degradation Test:

Samples were placed in vacuum oven at temperature 100°C, and then their mechanical properties were tested after being left in the oven for 2,4,7 and 14 days and compared to the samples at day zero following *ASTM 0573-9*.

4.4.2.1. Stress/Strain Measurements of thermally degraded samples:

4.4.2.1.1. Neat CA, PLA and PU:

Figure (4.26) showing stress strain curves of neat CA after samples at various durations in the oven at 100 °C. Namely, 0, 2, 4, 7 and 14 days. After two days in the oven, samples showed a decrease in both tensile elongation and nominal force. Nominal force showed a significant decrease by 260%. After 4 and 7 days, the decrease in both tensile elongation and nominal force continued. Nominal force showed a marked decrease by 357.6% and 390.9% after days 4 and 7 days respectively. At day 14, samples failed to be tested for their mechanical proerpties as the tested sample became extremely weak for testing.

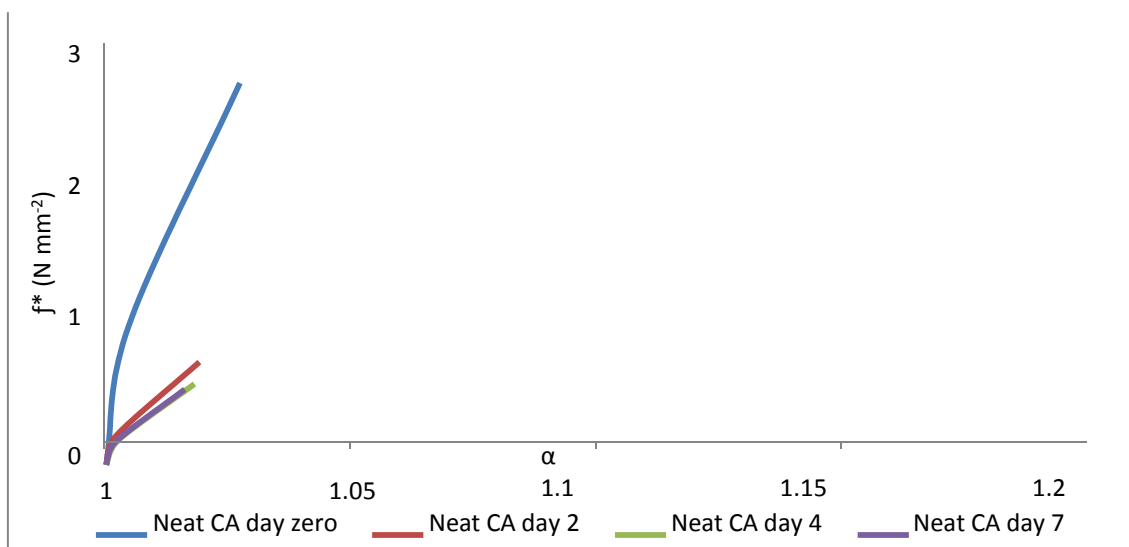


Figure 4.26 Stress-strain isotherm of dry thermal degradation test for neat CA

Figure (4.27) showed stress-strain curves for neat PLA at various durations in the oven at 100 °C. Namely, 0, 2, 4, 7 and 14 days. Samples showed a decrease in both tensile elongation and nominal force. A decrease in nominal force indicated by 8.5%, 22.5% and 40.7% for days 2, 4 and 7 respectively. Sample after 14 days have also failed to be tested. These results can be attributed to the influence of thermal degradation on the

aliphatic PLA chains which most probably took place easily at the ester groups along the polymeric backbone by random chain scission thus resulting in the hydrolysis and breakdown of the polymeric chains.

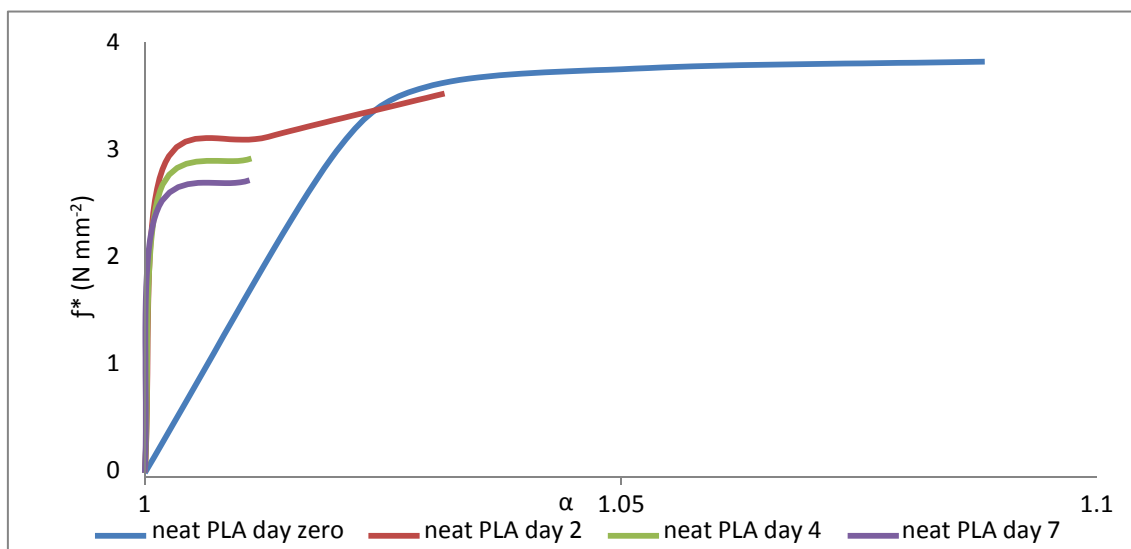


Figure 4.27 Stress-strain isotherm of dry thermal degradation test for neat PLA

Figure (4.28) shows stress strain curves of neat PU at various durations in the oven at 100°C namely, 0, 2, 4, 7 and 14 days. Samples showed an interesting finding, as samples showed an increase in both tensile elongation and nominal force at day 2. The increase in tensile elongation was by 3.1% and 2.9% for the nominal force. This can be explained due to the morphology of PU, as the hard segment content act as physical cross-links and reinforce the PU in a similar behavior as the nanofiller. Sample displayed elastomeric behavior, the crystallization induced phase separation starts around 60°C, and this explanation was stated in literature. (89) This transition changes the morphology of PU from fairly amorphous polymer above its glass transition temperature to a phase separated polymer with a domain structure. These domains act as physical cross links between the liquid chains which results in increasing the modulus. While at days 4, 7 and 14, the sample showed a decrease in both tensile elongation and nominal force. Day 14 showed the highest decrease by 26% in tensile elongation and 100% in nominal force.

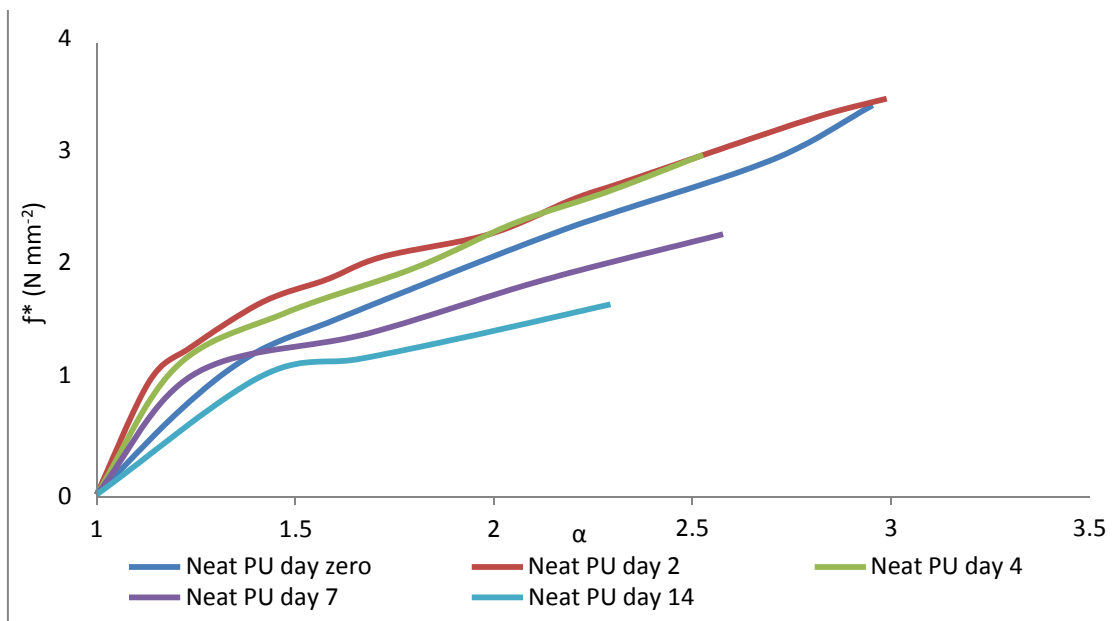


Figure 4.28 Stress-strain isotherm of dry thermal degradation test for neat PU

4.4.2.1.2. PLA/CA Composites:

Figure (4.29) shows stress strain curves for 60% PLA blend at various durations in the oven at 100°C. Namely, 0, 2, 4, 7 and 14 days. Blends with higher ratios of CA failed to be tested for their mechanical properties. Samples showed a decrease in both tensile elongation and nominal force. Decrease in nominal force was recorded by 17.6%, 33.3% and 81.8% for days 2, 4 and 7. These results can be attributed to thermal degradation of the aliphatic PLA chains. Sample at day 14 failed to be tested for its mechanical properties as it was completely degraded.

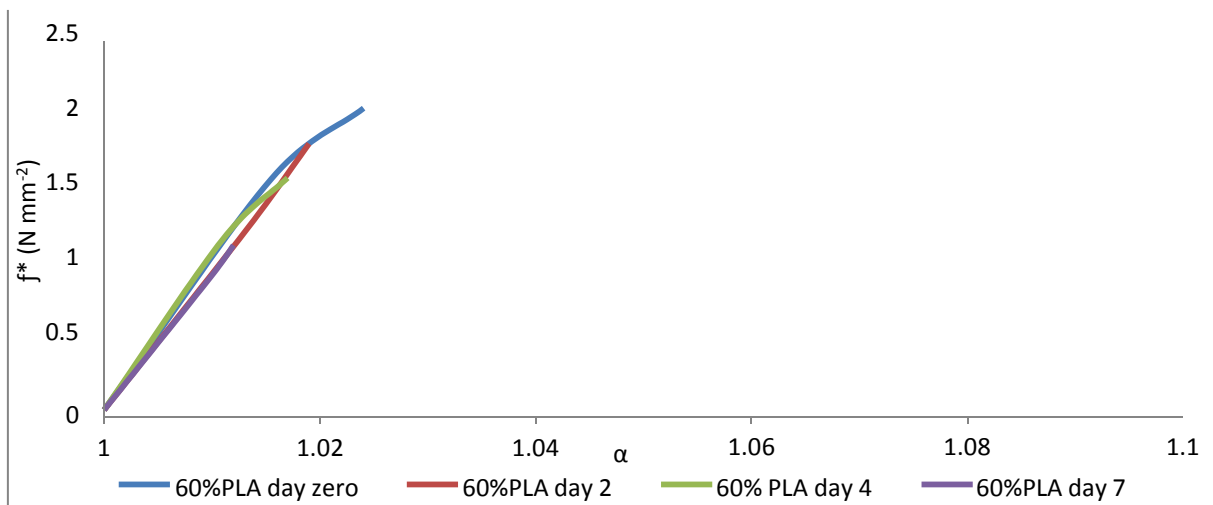


Figure 4.29 Stress-strain isotherm of dry thermal degradation test for blend of 60% PLA

4.4.2.1.3. PU/CA Composites:

Figure (4.30) shows stress strain curves for blend of 60% PU at various durations in the oven at 100°C. Namely, 0, 2, 4, 7 and 14 days. The characteristic behavior of PU that was reported previously continued to show in day 2 of this nanocomposite; an increase in both, tensile elongation and nominal force by 54.5% and 1.3% respectively, which is attributed to the presence of hard segments in PU as it shows elastomeric behavior which cause crystallization-induced phase separation which starts nearly at 60°C as recorded by. (89) These crystalline domains acts as physical cross- links between the liquid chains and increase the mechanical properties of the blend. Days 4, 7 and 14 showed a natural decrease in both tensile elongation and nominal force as expected. Day 14 showed the highest decrease in both values by 4.3% and 89% respectively.

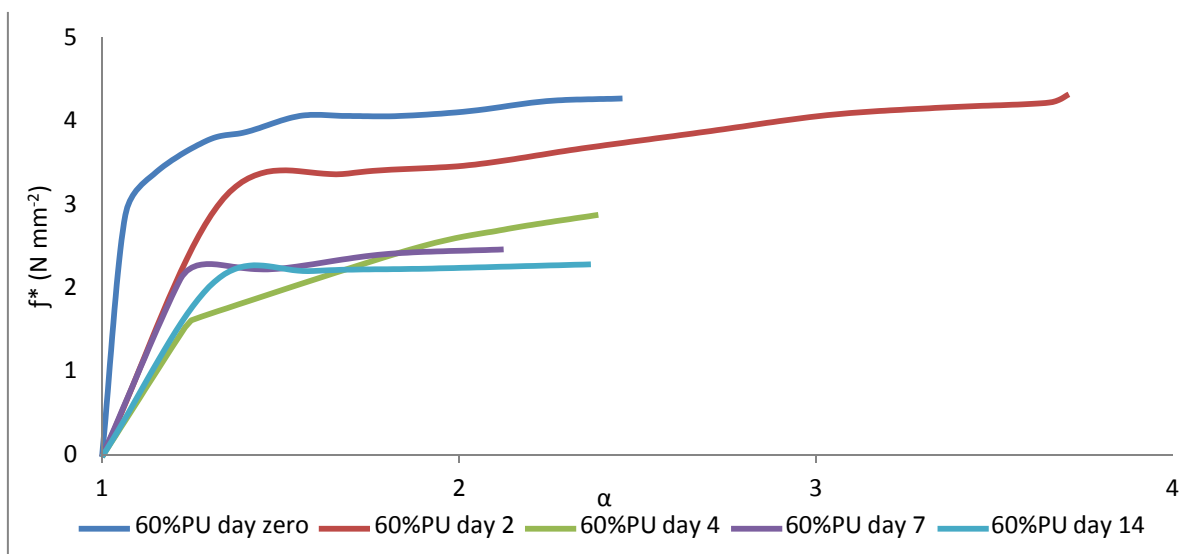


Figure 4.30 Stress strain curves of dry thermal degradation for blends of 60%PU

4.4.2.1.4. CA, PLA and PU with GnPs-COOH Nanocomposites:

Figure (4.31) shows stress strain curves of CA/GnPs-COOH at various durations in the oven at 100°C. Namely, 0, 2, 4, 7, and 14 days. Samples showed a decrease in both tensile elongation and nominal force. The presence of the nanofiller showed better stability for the samples when compared to the same samples without the nanofiller. The decrease in the nominal force was recorded to be 12.9%, 28%, 66.6% and 89% after 2, 4, 7 and 14 days, respectively. This relative stability can be explained due to the high thermal stability of GnPs-COOH high aspect ratio and ordered lamellar structure. Acting as an insulating surface and thus positively improving the overall thermal stability of the nanocomposite.

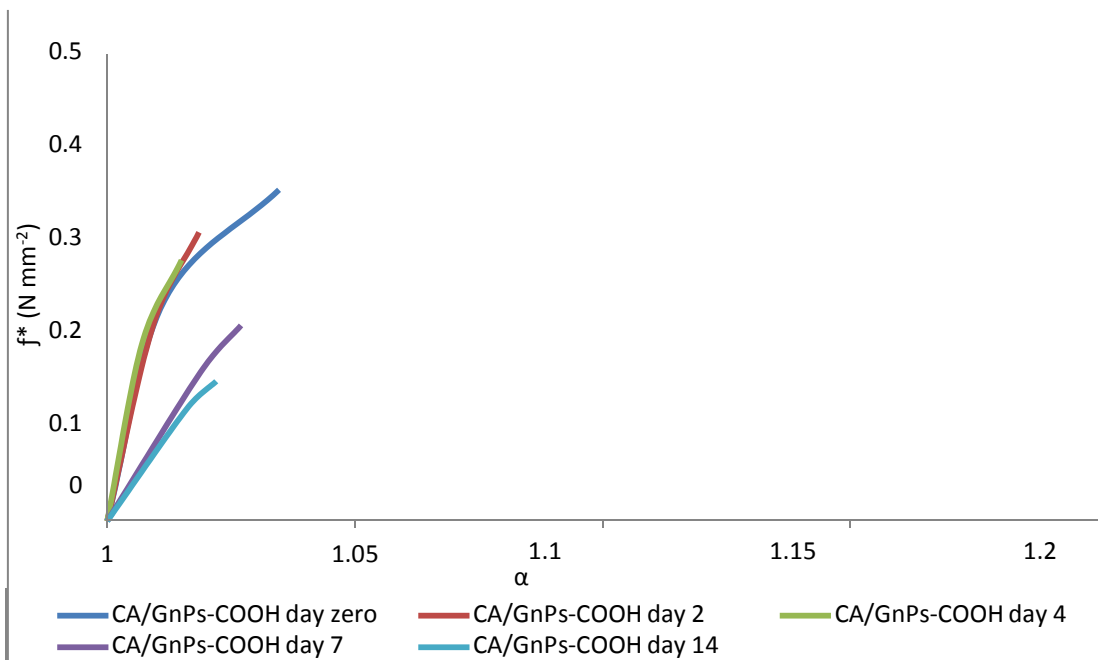


Figure 4.31 Stress-strain isotherm of dry thermal degradation test for CA/GnPs-COOH

Figure (4.32), showed stress strain curves for samples PLA/GnPs- COOH at various durations at oven at 100°C. Namely,0, 2, 4, 7 and 14 days. Samples showed a decrease in both tensile elongation and nominal force. Nominal force showed a decrease by 5.7%, 19.3% and 42.3% after 2, 4 and 7 days respectively. Sample at day 14 failed to be tested for its mechanical properties. This slight enhancement in the thermal stability of the nanocomposite can be attributed to the presence of the nanofiller, as GnPs- COOH act as an insulator for the nanocomposite.

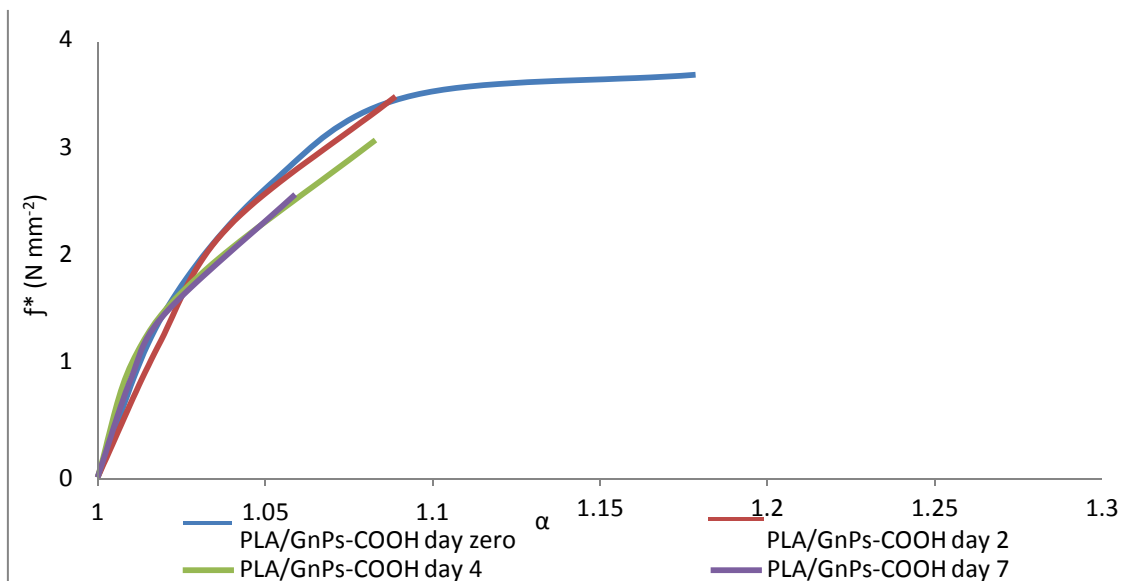


Figure 4.32 Stress-strain isotherm of dry thermal degradation test for PLA/GNPs-COOH

Figure (4.33) shows stress strain curves for PU/GnPS-COOH at various durations in the oven at 100°C. Namely, 0, 2, 4, 7 and 14 days. A significant increase of 39.6% and 7.5% for both tensile elongation and nominal force respectively was recorded at day 2. This can be attributed to the presence of the nanofiller as it enhanced the strength of the composite, as GnPS-COOH acts as an insulator which protects the composite from thermal degradation. In addition to the presence of the hard segments which results in phase separated structure as mentioned earlier. Days 4, 7 and 14 showed a natural decrease in the tensile elongation and nominal force. The highest decrease recorded at day 14 was 40.7% for the tensile elongation and 97% for the nominal force.

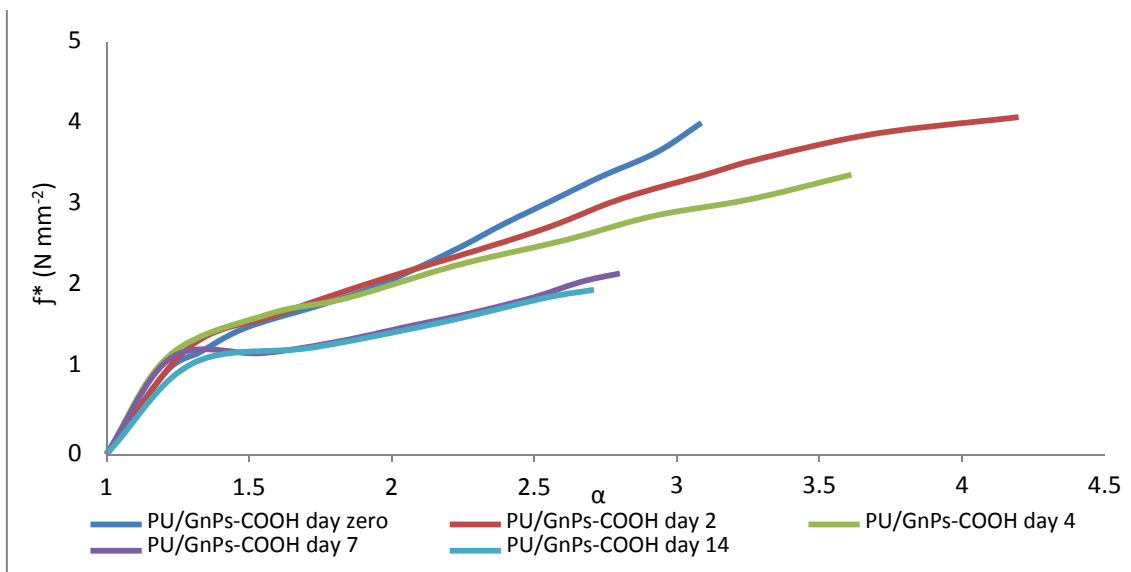


Figure 4.33 Stress-strain isotherm of dry thermal degradation test for PU/GNPS-COOH

4.4.2.1.5. PLA/CA/GnPs-COOH:

Figure (4.34) shows stress strain curves for 60%PLA/40%CA/GnPs- COOH nanocomposites at various durations in the oven at 100°C. Namely, 0, 2, 4, 7 and 14 days. As noted for other samples, a decrease in tensile elongation and nominal force were recorded for all durations. Nominal force showed a decrease by 9.3%, 26.5% and 57% for days 2, 4 and 7, respectively with the sample at day 14 failed to be tested for its mechanical properties

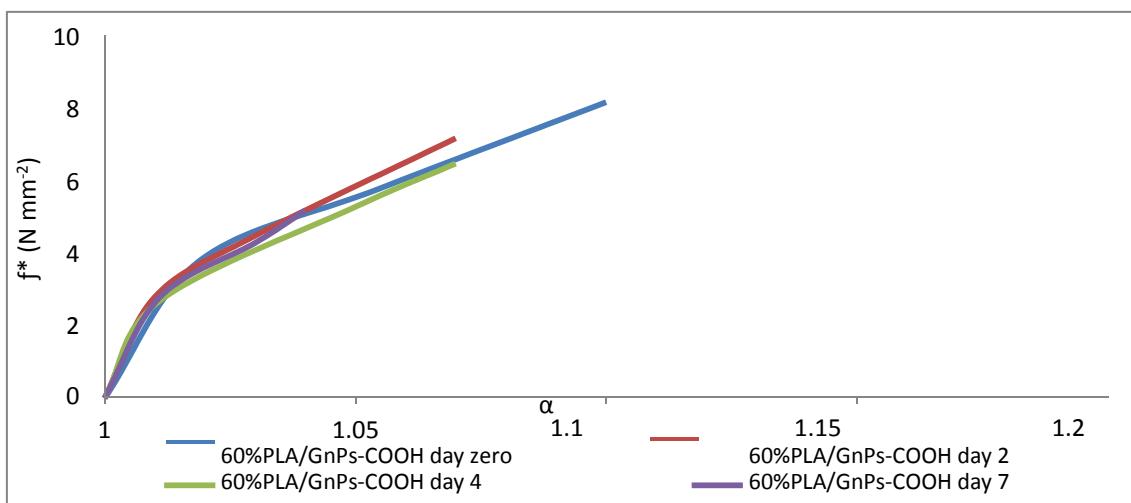


Figure 4.34 Stress-strain isotherm of dry thermal degradation test for 60%PLA/0.5wt%GnPS-COOH

4.4.2.1.6. PU/CA/GnPs-COOH:

Similar observations and discussions are also noted for 60% PU/GnPs-COOH nanocomposites as shown in *Figure 4.35* at various durations in the oven at 100°C. Namely, 0,2,4,7 and 14 days.

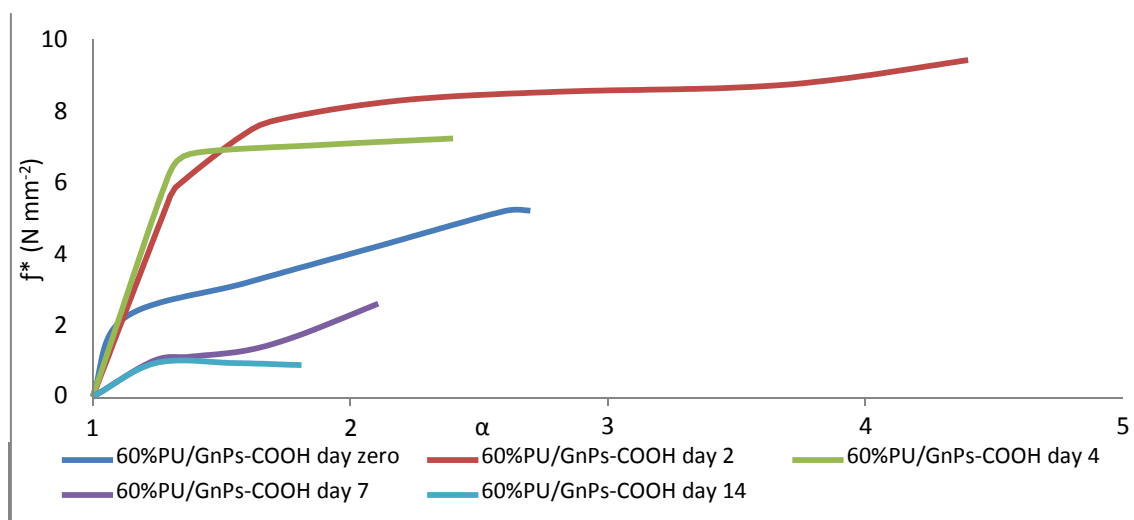


Figure 4.35 Stress-strain isotherm of dry thermal degradation test for 60% PU/GnPS-COOH

5. Conclusion and Future Work:

The aim of this work is to study the thermal and mechanical properties of CA, PLA and PU blends and nanocomposites. CA, PLA and PU are known to have desirable features represented in its biorenewability and biodegradability. However, the brittle nature of CA hinders its use in various applications. Thus, the first part of this thesis entailed adding other biopolymers such as PLA and PU to CA and to study the new various characteristics of the formed blends. Blends of CA/PLA at different ratios were examined. No enhancement in the mechanical properties was recorded for these blends probably due to the disparate hydrophilicities of both CA and PLA. On the other hand, the addition of PU to CA at different ratios showed an improvement in the mechanical properties due to the presence of hard and soft segments of PU which acts as a reinforcement as well as the full molecular interaction between CA and PU.

The second part, examines the incorporation of the nanofiller at constant concentration, 0.5wt%GNPS-COOH, to the blends and its effect on the mechanical and thermal properties of the formed nanocomposites. CA/PLA/GnPs-COOH nanocomposites showed an enhancement in the mechanical properties. This is due to the presence of hydrogen bonding between the carbonyl group of PLA and carboxylic group of GnPs- COOH. Maximum elongation, maximum nominal force and energy required to break the sample all increased at the ratios of 20%CA/80%PLA/GnPs-COOH. FT-IR analysis proved the hydrogen bonding in the nanocomposite. TGA analysis indicated an improved thermal stability of the nanocomposite. SEM micrographs showed a uniform distribution of the nanofiller in the matrices.

The incorporation of nanofiller to different ratios of CA/PU was studied. It showed an improvement in the mechanical properties of the nanocomposites. This improvement is due to the nano effect which relies on the interfacial area between the matrix and the nanofiller, as well as the extensive hydrogen bonding formed between the carboxylic group of nanofiller and carbonyl ester group of polymeric chains thus enhance the dispersion of nanofiller which was proved by FT-IR analysis.. Tensile elongation, maximum nominal force and energy required to break the sample all have shown an increase at the ratio of 20%CA/80%PU/GnPs- COOH. TGA analysis showed an enhancement in the thermal stability due to the

formed charred layer that prevent the permeation of oxygen due to high aspect and lamellar structure of the nanofiller. SEM images showed a uniform distribution of the nanofiller in the matrices.

Dry thermal degradation tests were carried out for all blends and nanocomposites. All samples showed complete degradation after thermal treatment for 14 days. The addition of the nanofiller particles to the blends improved the mechanical properties of the blends. In case of CA/PU blend, it showed a characteristic behavior after 2 days, as the mechanical properties were actually improved. This can be explained as the formation of a phase separated polymer with domain structure; which acts as physical cross links between liquid chains which results in increase in modulus. The blend then showed normal behavior and degradation at day 14. In case of CA/PU/GnPs-COOH, it continued to show the characteristic behavior at day 2 but with a more improved properties due to the presence of the nanofiller which acts as an insulator that protects the nanocomposite from degradation.

It was noticed that the incorporation of the nanofiller 0.5wt%GnPs-COOH have generally enhanced the mechanical and thermal properties of the nanocomposites making them excellent candidates for various applications such as food packaging, water desalination and automotives.

Further studies of this work may include the addition of plasticizers to PLA nanocomposites to enhance its elastic properties, to enhance the green sustainable society.

6. References:

1. Funabashi, Masahiro, Fumi Ninomiya, and Masao Masao Kunioka. "Biodegradability Evaluation of Polymers by ISO 14855-2." *IJMS International Journal of Molecular Sciences* 10.8 (2009): 3635-654
2. Mittal, Vikas. "Nanocomposites with Biodegradable Polymers." (2011): n. pag.
3. Siracusa, Valentina, Pietro Rocculi, Santina Romani, and Marco Dalla Rosa. "Biodegradable Polymers for Food Packaging: A Review." *Trends in Food Science & Technology* 19.12 (2008): 634-43.
4. Wang, Hui-Min, Yi-Ting Chou, Chin-San Wu, and Jen-Taut Yeh. "Polyester/cellulose Acetate Composites: Preparation, Characterization and Biocompatible." *Journal of Applied Polymer Science J. Appl. Polym. Sci.* 126.S2 (2012)
5. Yu, Long, and Ling Chen. "Polymeric Materials from Renewable Resources." *Biodegradable Polymer Blends and Composites from Renewable Resources Yu/Biodegradable Polymer Blends* (2008)
6. Ali, Fathilah Binti, Dong Jin Kang, Minsoo P. Kim, Chul-Hee Cho, and Bumjoon J. Kim. "Synthesis of Biodegradable and Flexible, Polylactic Acid Based, Thermoplastic
7. Auras, R. A., B. Harte, S. Selke, and R. Hernandez. "Mechanical, Physical, and Barrier Properties of Poly(Lactide) Films." *Journal of Plastic Film and Sheeting* 19.2 (2003):
8. Brito, Luciana M., Fabián Vaca Chávez, Maria Inês Bruno Tavares, and Pedro J.o. Sebastião. "Molecular Dynamic Evaluation of Starch-PLA Blends Nanocomposite with Organoclay by Proton NMR Relaxometry." *Polymer Testing* 32.7 (2013)
9. Chen, Jin Zhou, Zhen Gao, Peng Ping Xie, Kai Guo, Ming Jun Niu, and Xin Fa Li. "Preparation and Characterization of Polylactic Acid/Acetate Starch Blends with Tetrabutyl Titanate." *AMR Advanced Materials Research* 284-286 (2011)
10. Ke, Tianyi, and Xiuzhi Sun. "Effects of Moisture Content and Heat Treatment on the Physical Properties of Starch and Poly(lactic Acid) Blends." *Journal of Applied Polymer Science J. Appl. Polym. Sci.* 81.12 (2001): 3069-082.
11. Mitchell, M. R., R. E. Link, Mu-Hoe Yang, and Yeuh-Hui Lin. "Measurement and Simulation of Thermal Stability of Poly(Lactic Acid) by Thermogravimetric Analysis." *Journal of Testing and Evaluation J. Test. Eval.* 37.4 (2009): 102271.
12. Müller, Carmen M. O., Alfredo T. N. Pires, and Fabio Yamashita. "Characterization of Thermoplastic Starch/poly(lactic Acid) Blends Obtained by Extrusion and Thermopressing." *J. Braz. Chem. Soc. Journal of the Brazilian Chemical Society* (2012): n. pag.
13. Nampoothiri, K. Madhavan, Nimisha Rajendran Nair, and Rojan Pappy John. "An Overview of the Recent Developments in Polylactide (PLA) Research." *Bioresource Technology* 101.22 (2010): 8493-501
14. Xiong, Zhu, Yong Yang, Jianxiang Feng, Xiaomin Zhang, Chuanzhi Zhang, Zhaobin Tang, and Jin Zhu. "Preparation and Characterization of Poly(lactic Acid)/starch

- Composites Toughened with Epoxidized Soybean Oil." *Carbohydrate Polymers* 92.1 (2013)
15. Yokesahachart, Chanakorn, and Rangrong Yoksan. "Effect of Amphiphilic Molecules on Characteristics and Tensile Properties of Thermoplastic Starch and Its Blends with Poly(lactic Acid)." *Carbohydrate Polymers* 83.1 (2011): 22-31.
 16. Zhang, Jian-Feng, and Xiuzhi Sun. "Mechanical and Thermal Properties of Poly(lactic Acid)/starch Blends with Dioctyl Maleate." *Journal of Applied Polymer Science J. Appl. Polym. Sci.* 94.4 (2004):
 17. Qu, Wen-Qiang, Yi-Ran Xia, Li-Juan Jiang, Li-Wei Zhang, and Zhao-Sheng Hou. "Synthesis and Characterization of a New Biodegradable Polyurethanes with Good Mechanical Properties." *Chinese Chemical Letters* 27.1 (2016): 135-38.
 18. Runumi Gogoi. "Effect Of Soft Segment Chain Length On Tailoring The Properties Of Isocyanate Terminated Polyurethane Prepolymer, A Base Material For Polyurethane Bandage". *International Journal of Research in Engineering and Technology IJRET* 02.10 (2013): 395-98.
 19. Runumi Gogoi. "Effect Of Soft Segment Chain Length On Tailoring The Properties Of Isocyanate Terminated Polyurethane Prepolymer, A Base Material For Polyurethane Bandage". *International Journal of Research in Engineering and Technology IJRET* 02.10 (2013): 395-98.
 21. Weng, Shengguang, Zhean Xia, Jianding Chen, and Luanluan Gong. "Shape Memory Properties of Polycaprolactone-based Polyurethanes Prepared by Reactive Extrusion." *Journal of Applied Polymer Science J. Appl. Polym. Sci.* 127.1 (2013)
 22. Zavastin, Daniela, Igor Cretescu, Mariana Bezdadea, Militina Bourceanu, Maria Drăgan, Gabriela Lisa, Ionel Mangalagiu, Vesna Vasić, and Jasmina Savić. "Preparation, Characterization and Applicability of Cellulose Acetate–polyurethane Blend Membrane in Separation Techniques." *Colloids and Surfaces A: Physicochemical and Engineering Aspects* 370.1-3 (2010): 120-28.
 23. Taha, Ahmed A., Yi-Na Wu, Hongtao Wang, and Fengting Li. "Preparation and Application of Functionalized Cellulose Acetate/silica Composite Nanofibrous Membrane via Electrospinning for Cr(VI) Ion Removal from Aqueous Solution." *Journal of Environmental Management* 112 (2012): 10-16.
 24. Spinella, Stephen, Giada Lo Re, Bo Liu, John Dorgan, Youssef Habibi, Jean-Marie Raquez, Philippe Dubois, and Richard A. Gross. "Modification of Cellulose Nanocrystals with Lactic Acid for Direct Melt Blending with PLA." (2015): n. pag.
 25. Pinto, V.c., Tiago Ramos, Sofia Alves, J. Xavier, Paulo Tavares, P.m.g.p. Moreira, and Rui Miranda Guedes. "Comparative Failure Analysis of PLA, PLA/GNP and PLA/CNT-

- COOH Biodegradable Nanocomposites Thin Films." *Procedia Engineering* 114 (2015): 635-42
26. Chang, Dong Wook, Hyun-Jung Choi, In-Yup Jeon, and Jong-Beom Baek. "Edge-Selectively Functionalized Graphene Nanoplatelets." *The Chemical Record* 13.2 (2013)
 27. Chieng, Buong Woei, Nor Azowa Ibrahim, Wan Md Zin Wan Yunus, Mohd Zobir Hussein, and Yuet Ying Loo. "Effect of Graphene Nanoplatelets as Nanofiller in Plasticized Poly(lactic Acid) Nanocomposites." *J Therm Anal Calorim Journal of Thermal Analysis and Calorimetry* 118.3 (2014): 1551-559.
 28. Chieng, Buong, Nor Ibrahim, Wan Yunus, Mohd Hussein, Yoon Then, and Yuet Loo. "Effects of Graphene Nanoplatelets and Reduced Graphene Oxide on Poly(lactic Acid) and Plasticized Poly(lactic Acid): A Comparative Study." *Polymers* 6.8 (2014)
 29. Galpaya, Dilini, Mingchao Wang, Meinan Liu, Nunzio Motta, Eric Waclawik, and Cheng Yan. "Recent Advances in Fabrication and Characterization of Graphene-Polymer Nanocomposites." *Graphene* 01.02 (2012)
 30. Parashar, Avinash, and Pierre Mertiny. "Multiscale Model to Investigate the Effect of Graphene on the Fracture Characteristics of Graphene/polymer Nanocomposites." *Nanoscale Research Letters* 7.1 (2012)
 31. Shen, Yuxia, Tao Jing, Weijie Ren, Jiewei Zhang, Zhi-Guo Jiang, Zhong-Zhen Yu, and Aravind Dasari. "Chemical and Thermal Reduction of Graphene Oxide and Its Electrically Conductive Polylactic Acid Nanocomposites." *Composites Science and Technology* 72.12 (2012): 1430-435.
 32. Jeon, In-Yup, Hyun-Jung Choi, Sun-Min Jung, Jeong-Min Seo, Min-Jung Kim, Liming Dai, and Jong-Beom Baek. "Large-Scale Production of Edge-Selectively Functionalized Graphene Nanoplatelets via Ball Milling and Their Use as Metal-Free Electrocatalysts for Oxygen Reduction Reaction." *J. Am. Chem. Soc. Journal of the American Chemical Society* 135.4 (2013): 1386-393.
 33. Jiang, Xian, and Lawrence T. Drzal. "Reduction in Percolation Threshold of Injection Molded High-density Polyethylene/exfoliated Graphene Nanoplatelets Composites by Solid State Ball Milling and Solid State Shear Pulverization." *Journal of Applied Polymer Science J. Appl. Polym. Sci.* 124.1 (2011): 525-35.
 34. Kavan, Ladislav, Jun-Ho Yum, and Michael Grätzel. "Graphene Nanoplatelets Outperforming Platinum as the Electrocatalyst in Co-Bipyridine-Mediated Dye-Sensitized Solar Cells." *Nano Letters Nano Lett.* 11.12 (2011): 5501-506
 35. Mehrali, Mohammad, Sara Tahan Latibari, Mehdi Mehrali, Teuku Meurah Indra Mahlia, Hendrik Simon Cornelis Metselaar, Mohammad Sajad Naghavi, Emad Sadeghinezhad, and Amir Reza Akhiani. "Preparation and Characterization of Palmitic Acid/graphene Nanoplatelets Composite with Remarkable Thermal Conductivity as a Novel Shape-stabilized Phase Change Material." *Applied Thermal Engineering* 61.2 (2013): 633-40.
 36. Qin, Wenzhen, Frederic Vautard, Lawrence T. Drzal, and Junrong Yu. "Mechanical and Electrical Properties of Carbon Fiber Composites with Incorporation of Graphene

- Nanoplatelets at the Fiber–matrix Interphase." *Composites Part B: Engineering* 69 (2015): 335-41
37. Rosenzweig, Shirley, George A. Sorial, Endalkachew Sahle-Demessie, and Drew C. Mcavoy. "Optimizing the Physical-chemical Properties of Carbon Nanotubes (CNT) and Graphene Nanoplatelets (GNP) on Cu(II) Adsorption." *Journal of Hazardous Materials* 279 (2014): 410-17
 38. Saravanan, N., R. Rajasekar, S. Mahalakshmi, T. Sathishkumar, K. Sasikumar, and S. Sahoo. "Graphene and Modified Graphene-based Polymer Nanocomposites - A Review." *Journal of Reinforced Plastics and Composites* 33.12 (2014): 1158-170.
 39. Zavastin, Daniela, Igor Cretescu, Mariana Bezdadea, Militina Bourceanu, Maria Drăgan, Gabriela Lisa, Ionel Mangalagiu, Vesna Vasić, and Jasmina Savić. "Preparation, Characterization and Applicability of Cellulose Acetate–polyurethane Blend Membrane in Separation Techniques." *Colloids and Surfaces A: Physicochemical and Engineering Aspects* 370.1-3 (2010): 120-28.
 40. Chatterjee, Sanjukta. *Structural and Physical Effects of Carbon Nanofillers in Thermoplastic and Thermosetting Polymer Systems*. Uppsala: Acta Universitatis Upsaliensis, 2012
 41. Chieng, Buong, Nor Ibrahim, Wan Yunus, Mohd Hussein, Yoon Then, and Yuet Loo. "Effects of Graphene Nanoplatelets and Reduced Graphene Oxide on Poly(lactic Acid) and Plasticized Poly(lactic Acid): A Comparative Study." *Polymers* 6.8 (2014)
 42. Galpaya, Dilini, Mingchao Wang, Meinan Liu, Nunzio Motta, Eric Waclawik, and Cheng Yan. "Recent Advances in Fabrication and Characterization of Graphene-Polymer Nanocomposites." *Graphene* 01.02 (2012)
 43. Parashar, Avinash, and Pierre Mertiny. "Multiscale Model to Investigate the Effect of Graphene on the Fracture Characteristics of Graphene/polymer Nanocomposites." *Nanoscale Research Letters* 7.1 (2012)
 44. Ahmadi-Moghadam, B., M. Sharafimasooleh, S. Shadlou, and F. Taheri. "Effect of Functionalization of Graphene Nanoplatelets on the Mechanical Response of Graphene/epoxy Composites." *Materials & Design* 66 (2015): 142-49.
 45. Chatterjee, S., F. Nafezarefi, N.h. Tai, L. Schlagenhauf, F.a. Nüesch, and B.t.t. Chu. "Size and Synergy Effects of Nanofiller Hybrids including Graphene Nanoplatelets and Carbon Nanotubes in Mechanical Properties of Epoxy Composites." *Carbon* 50.15 (2012): 5380-386
 46. Chieng, Buong Woei, Nor Azowa Ibrahim, Wan Md Zin Wan Yunus, Mohd Zobir Hussein, and Yuet Ying Loo. "Effect of Graphene Nanoplatelets as Nanofiller in Plasticized Poly(lactic Acid) Nanocomposites." *J Therm Anal Calorim Journal of Thermal Analysis and Calorimetry* 118.3 (2014): 1551-559.
 47. Domun, N., H. Hadavinia, T. Zhang, T. Sainsbury, G. H. Liaghat, and S. Vahid. "Improving the Fracture Toughness and the Strength of Epoxy Using Nanomaterials – a Review of the Current Status." *Nanoscale* 7.23 (2015): 10294-0329.

48. Balakrishnan, Harintharavimal, Azman Hassan, Mat Uzir Wahit, A.a. Yussuf, and Shamsul Bahri Abdul Razak. "Novel Toughened Polylactic Acid Nanocomposite: Mechanical, Thermal and Morphological Properties." *Materials & Design* 31.7 (2010): 3289-298.
49. Brito, Luciana M., Fabián Vaca Chávez, Maria Inês Bruno Tavares, and Pedro J.o. Sebastião. "Molecular Dynamic Evaluation of Starch-PLA Blends Nanocomposite with Organoclay by Proton NMR Relaxometry." *Polymer Testing* 32.7 (2013)
50. Chieng, Buong Woei, Nor Azowa Ibrahim, Wan Md Zin Wan Yunus, Mohd Zobir Hussein, and Yuet Ying Loo. "Effect of Graphene Nanoplatelets as Nanofiller in Plasticized Poly(lactic Acid) Nanocomposites." *J Therm Anal Calorim Journal of Thermal Analysis and Calorimetry* 118.3 (2014)
51. Hassan, Elwathig, You Wei, He Jiao, and Muhuo Yu. "Dynamic Mechanical Properties and Thermal Stability of Poly(lactic Acid) and Poly(butylene Succinate) Blends Composites." *Journal of Fiber Bioengineering and Informatics JFBI* 6.1 (2013): 85-94.
52. Gunaratne, L.m. Wasantha K., and R.a. Shanks. "Miscibility, Melting, and Crystallization Behavior of Poly(hydroxybutyrate) and Poly(D,L-lactic Acid) Blends." *Polym. Eng. Sci. Polymer Engineering & Science* 48.9 (2008): 1683-692.
53. Cai, Dongyu, Jie Jin, Kamal Yusoh, Rehman Rafiq, and Mo Song. "High Performance Polyurethane/functionalized Graphene Nanocomposites with Improved Mechanical and Thermal Properties." *Composites Science and Technology* 72.6 (2012)
54. Imre, Balázs, Dániel Bedő, Attila Domján, Peter Schön, G. Julius Vancso, and Béla Pukánszky. "Structure, Properties and Interfacial Interactions in Poly(lactic Acid)/polyurethane Blends Prepared by Reactive Processing." *European Polymer Journal* 49.10 (2013)
55. Kojio, Ken, Mutsuhisa Furukawa, Yoshiteru Nonaka, and Sadaharu Nakamura. "Control of Mechanical Properties of Thermoplastic Polyurethane Elastomers by Restriction of Crystallization of Soft Segment." *Materials* 3.12 (2010): 5097-110.
56. Raghu, Anjanapura V., Yu Rok Lee, Han Mo Jeong, and Cheol Min Shin. "Preparation and Physical Properties of Waterborne Polyurethane/Functionalized Graphene Sheet Nanocomposites." *Macromol. Chem. Phys. Macromolecular Chemistry and Physics* 209.24 (2008)
57. Lai, S.-M., and Y.-C. Lan. "Shape Memory Properties of Melt-blended Polylactic Acid (PLA)/thermoplastic Polyurethane (TPU) Bio-based Blends." *Journal of Polymer Research J Polym Res* 20.5 (2013)
58. Bitinis, Natacha, Raquel Verdejo, Julien Bras, Elena Fortunati, Jose Maria Kenny, Luigi Torre, and Miguel Angel López-Manchado. "Poly(lactic Acid)/natural Rubber/cellulose Nanocrystal Bionanocomposites Part I. Processing and Morphology." *Carbohydrate Polymers* 96.2 (2013): 611-20.

59. Shumigin, Dmitri, Elvira Tarasova, Andres Krumme, and Pille Meier. "Rheological and Mechanical Properties of Poly(lactic) Acid/Cellulose and LDPE/Cellulose Composites." *Ms Materials Science* 17.1 (2011)
60. Robles, Eduardo, Iñaki Urruzola, Jalel Labidi, and Luis Serrano. "Surface-modified Nano-cellulose as Reinforcement in Poly(lactic Acid) to Conform New Composites." *Industrial Crops and Products* 71 (2015): 44-53.
61. Kuvardina, E. V., L. A. Novokshonova, S. M. Lomakin, S. A. Timan, and I. A. Tchmutin. "Effect of the Graphite Nanoplatelet Size on the Mechanical, Thermal, and Electrical Properties of Polypropylene/exfoliated Graphite Nanocomposites." *Journal of Applied Polymer Science J. Appl. Polym. Sci.* (2012): n. pag
62. Polschikov, Sergey V., Polina M. Nedorezova, Alla N. Klyamkina, Anton A. Kovalchuk, Alexander M. Aladyshv, Alexander N. Shchegolikhin, Vitaliy G. Shevchenko, and Vyacheslav E. Muradyan. "Composite Materials of Graphene Nanoplatelets and Polypropylene, Prepared by in Situ Polymerization." *Journal of Applied Polymer Science J. Appl. Polym. Sci.* 127.2 (2012): 904-11
63. Fu, Yu, Linshu Liu, and Jinwen Zhang. "Manipulating Dispersion and Distribution of Graphene in PLA through Novel Interface Engineering for Improved Conductive Properties." *ACS Appl. Mater. Interfaces ACS Applied Materials & Interfaces* 6.16 (2014): 14069-4075.
64. Cai, Dongyu, Jie Jin, Kamal Yusoh, Rehman Rafiq, and Mo Song. "High Performance Polyurethane/functionalized Graphene Nanocomposites with Improved Mechanical and Thermal Properties." *Composites Science and Technology* 72.6 (2012)
65. Liu, Jen-Chieh, Darren J. Martin, Robert J. Moon, and Jeffrey P. Youngblood. "Enhanced Thermal Stability of Biomedical Thermoplastic Polyurethane with the Addition of Cellulose Nanocrystals." *Journal of Applied Polymer Science J. Appl. Polym. Sci.* 132.22 (2015): n. pag
66. Wang, Chengshuang, Yuge Zhang, Ling Lin, Liang Ding, Juan Li, Rong Lu, Meng He, Hongfeng Xie, and Rongshi Cheng. "Thermal, Mechanical, and Morphological Properties of Functionalized Graphene-reinforced Bio-based Polyurethane Nanocomposites." *European Journal of Lipid Science and Technology Eur. J. Lipid Sci. Technol.* (2015)
67. Yadav, Santosh Kumar, and Jae Whan Cho. "Functionalized Graphene Nanoplatelets for Enhanced Mechanical and Thermal Properties of Polyurethane Nanocomposites." *Applied Surface Science* 266 (2013): 360-67
68. Balakrishnan, Harinthaavimal, Azman Hassan, Mat Uzir Wahit, A.a. Yussuf, and Shamsul Bahri Abdul Razak. "Novel Toughened Polylactic Acid Nanocomposite: Mechanical, Thermal and Morphological Properties." *Materials & Design* 31.7 (2010): 3289-298.

69. Brito, Luciana M., Fabián Vaca Chávez, Maria Inês Bruno Tavares, and Pedro J.o. Sebastião. "Molecular Dynamic Evaluation of Starch-PLA Blends Nanocomposite with Organoclay by Proton NMR Relaxometry." *Polymer Testing* 32.7 (2013)
70. Chieng, Buong Woei, Nor Azowa Ibrahim, Wan Md Zin Wan Yunus, Mohd Zobir Hussein, and Yuet Ying Loo. "Effect of Graphene Nanoplatelets as Nanofiller in Plasticized Poly(lactic Acid) Nanocomposites." *J Therm Anal Calorim Journal of Thermal Analysis and Calorimetry* 118.3 (2014)
71. Gopiraman, M. "Structural and Mechanical Properties of Cellulose Acetate/graphene Hybrid Nanofibers: Spectroscopic Investigations." *Expresspolymlett Express Polymer Letters* 7.6 (2013): 554-63.
72. Martin, O., and L. Avérous. "Poly(lactic Acid): Plasticization and Properties of Biodegradable Multiphase Systems." *Polymer* 42.14 (2001): 6209-219.
73. Dai, Lin, Lu-Ying Wang, Tong-Qi Yuan, and Jing He. "Study on Thermal Degradation Kinetics of Cellulose-graft-poly(l-lactic Acid) by Thermogravimetric Analysis." *Polymer Degradation and Stability* 99 (2014)
75. Fu, Yu, Linshu Liu, and Jinwen Zhang. "Manipulating Dispersion and Distribution of Graphene in PLA through Novel Interface Engineering for Improved Conductive Properties." *ACS Appl. Mater. Interfaces ACS Applied Materials & Interfaces* 6.16 (2014): 14069-4075.
76. Halász, Katalin, and Levente Csóka. "Plasticized Biodegradable Poly(lactic Acid) Based Composites Containing Cellulose in Micro- and Nanosize." *Journal of Engineering* 2013
77. Bitinis, Natacha, Raquel Verdejo, Julien Bras, Elena Fortunati, Jose Maria Kenny, Luigi Torre, and Miguel Angel López-Manchado. "Poly(lactic Acid)/natural Rubber/cellulose Nanocrystal Bionanocomposites Part I. Processing and Morphology." *Carbohydrate Polymers* 96.2 (2013): 611-20.
78. Dai, Lin, Lu-Ying Wang, Tong-Qi Yuan, and Jing He. "Study on Thermal Degradation Kinetics of Cellulose-graft-poly(l-lactic Acid) by Thermogravimetric Analysis." *Polymer Degradation and Stability* 99 (2014)
79. Herrera, Natalia, Aji P. Mathew, and Kristiina Oksman. "Plasticized Polylactic Acid/cellulose Nanocomposites Prepared Using Melt-extrusion and Liquid Feeding: Mechanical, Thermal and Optical Properties." *Composites Science and Technology* 106 (2015): 149-55.
80. Jeon, Gil Woo, Ji-Eun An, and Young Gyu Jeong. "High Performance Cellulose Acetate Propionate Composites Reinforced with Exfoliated Graphene." *Composites Part B: Engineering* 43.8 (2012): 3412-418.

81. Jeon, Gil Woo, Ji-Eun An, and Young Gyu Jeong. "High Performance Cellulose Acetate Propionate Composites Reinforced with Exfoliated Graphene." *Composites Part B: Engineering* 43.8 (2012): 3412-418.
82. Gopiraman, M. "Structural and Mechanical Properties of Cellulose Acetate/graphene Hybrid Nanofibers: Spectroscopic Investigations." *Expresspolymlett Express Polymer Letters* 7.6 (2013): 554-63.
83. Kamal, H., F.m. Abd-Elrahim, and S. Lotfy. "Characterization and Some Properties of Cellulose Acetate-co-polyethylene Oxide Blends Prepared by the Use of Gamma Irradiation." *Journal of Radiation Research and Applied Sciences* 7.2 (2014): 146-53.
84. Liu, Lei, Zhigang Shen, Shuaishuai Liang, Min Yi, Xiaojing Zhang, and Shulin Ma. "Enhanced Atomic Oxygen Erosion Resistance and Mechanical Properties of Graphene/cellulose Acetate Composite Films." *Journal of Applied Polymer Science J. Appl. Polym. Sci.* 131.11 (2013):
85. Martin, O., and L. Avérous. "Poly(lactic Acid): Plasticization and Properties of Biodegradable Multiphase Systems." *Polymer* 42.14 (2001): 6209-219.
86. Wang, Fuzhong, Lawrence T. Drzal, Yan Qin, and Zhixiong Huang. "Multifunctional Graphene Nanoplatelets/cellulose Nanocrystals Composite Paper." *Composites Part B: Engineering* 79 (2015): 521-29.
87. Zhang, Xiaomin, Xiaoqing Liu, Wenge Zheng, and Jin Zhu. "Regenerated Cellulose/graphene Nanocomposite Films Prepared in DMAC/LiCl Solution." *Carbohydrate Polymers* 88.1 (2012): 26-30.
88. Robles, Eduardo, Iñaki Urruzola, Jalel Labidi, and Luis Serrano. "Surface-modified Nano-cellulose as Reinforcement in Poly(lactic Acid) to Conform New Composites." *Industrial Crops and Products* 71 (2015): 44-53.
89. Swolfs, Y., E. Bertels, I. Verpoest, and B. Goderis. "Linking the Morphology of a High Hard Segment Content Polyurethane to Its Thermal Behaviour and Mechanical Properties." *Polymer* 81 (2015): 1-11.